2016

Behavior of Light in a Photobioreactor and Design of Light Guides

Anand Rajendran
South Dakota State University

BEHAVIOR OF LIGHT IN A PHOTOBIOREACTOR AND DESIGN OF LIGHT GUIDES

BY

ANAND RAJENDRAN

A thesis submitted in partial fulfillment of the requirements for the

Master of Science

Major in Agricultural and Biosystems Engineering

South Dakota State University

2016

BEHAVIOR OF LIGHT IN A PHOTOBIOREACTOR AND

DESIGN OF LIGHT GUIDES

This thesis is approved as a creditable and independent investigation by a candidate for the Master of Science in Agricultural and Biosystems Engineering degree and is acceptable for meeting the thesis requirements for this degree. Acceptance of this thesis does not imply that the conclusions reached by the candidate are necessarily the conclusions of the major department.

Gary Anderson, Ph.D.
Major and Thesis Advisor Date

Van Kelley, Ph.D.
Head, Department of Agricultural and Biosystems Engineering Date

Dean, Graduate School Date

I would like to dedicate this thesis work to my parents and friends.

ACKNOWLEDGEMENTS

I would like to acknowledge my advisor and mentor Dr. Gary Anderson, for his constant support in accomplishing the research work.

I would like to thank my committee members, Dr. Larry Browning, Dr. Zhengrong Gu, and Dr. Renee Oscarson for their valuable suggestions, time and support whenever I required it.

Finally, I want to thank my parents, my wife, friends and family for their continuous support in achieving what I am today.

CONTENTS

ABBREVIATIONS

PBR	Photobioreactor
PAR	Photosynthetic active radiation
ATP	Adenosine triphosphate
ADP	Adenosine diphosphate
NADHP	Nicotinamide adenine dinucleotide phosphate (reduced form)
LHC	Light harvesting chlorophyll
TIR	Total internal reflection
PPFD	Photosynthetic photon flux density, μmol $m^{-2}s^{-1}$

LIST OF FIGURES

LIST OF TABLES

ABSTRACT

BEHAVIOR OF LIGHT IN A PHOTOBIOREACTOR AND

DESIGN OF LIGHT GUIDES

ANAND RAJENDRAN

2016

The purposes of the thesis is to explain the microalgae cultivation in a photobioreactor system; demonstrate the light activity in a flat-plate photobioreactor; and design the light channeling system.

Generally, microalgae are cultivated in open ponds and in closed photobioreactor systems. In open ponds, the productivity of microalgal biomass is very low, due to lack and improper use of carbon and energy sources. In photobioreactor systems, all required inputs can be supplied effectively to the microalgae which in turn increases the biomass productivity. However, these systems are expensive to build and to maintain in a large-scale basis. In a photobioreactor, the supply of carbon source can be controlled easily, but not the supply of energy. The main energy source in a photobioreactor is light. Controlling light activity in a photobioreactor can be a big challenge.

Since light plays a vital role in microalgal growth, studying light activity in a photobioreactor is crucial. The fundamentals of light behavior is also presented. An experiment has been carried out to analyze the interaction of light with all the factors like growth medium, gas bubble flumes, biomass concentration, and the light path length in the photobioreactor system. These experiments are used to determine the light penetration in to a photobioreactor system.

It is concluded that the light attenuates 15.80% to 44.83% across the light pathlength (101mm to 305mm); 7.045 to 36.6% with gas bubble flow rates (1 to 10 l/min); and 64.18% to 99.2% with the biomass concentration of (0 to 1 kg/m^3) in a photobioreactor system. The equations were developed to show the relation between output light intensity with three design factors. Therefore, the extinction coefficient is found to be $2m^{-1}$ for light path length, 0.41 min/m^4 for gas bubbles, and 58.44 m^2/kg for biomass concentration.

Different types of light guides were designed and tested for their photon transmission efficiency. Diameter, length and output taper angles are taken as design factors. The highest transmission efficiency of 90.17% is found in simple light guide of 102mm long and 50.8 mm diameter with 90° exit surface whereas the lowest transmission efficiency of 51.97% is found in light guide of 203 mm long and 9.53 mm diameter with a 60° exit surface.

.

1. INTRODUCTION

The depletion of non-renewable fossil fuel resources creates a need for an alternate fuel resource in the world which leads to the discovery of biofuels. Biofuels are considered as the potential alternate renewable fuel resource. They are commonly produced from terrestrial agricultural crops such as soybeans, rapeseed oil, oil palm, sugarcane, maize, sugar beet, etc. The production of biofuel from agricultural crops takes land area which affect the food security. Hence, the other alternate biofuel resource was sought and found to be aquatic microbial oxygenic photoautotrophs, which are cyanobacteria, algae and diatoms (Dismukes, Carrieri, Bennette, Ananyev, & Posewitz, 2008). Biomass produced from these organisms are a good source of non-saturated fatty acids or lipids and biomass (starch and glycogen) for fermentation. These products can be used to produce biofuel, animal feed, high-value pharmaceutical products, etc.

Biofuel can possibly displace the fossil fuel but it is not yet attainable, feasible and economically viable because of many limitations such as high land area requirement, high demand of agricultural crops, technological limitations, and high production cost and maintenance cost. Technologies on the production of biofuel from microalgae are still evolving.

Microalgae are considered as the potential resource for biofuel production because they take less land. Besides, the productivity is also high when compared to the productivity of biofuel from terrestrial crops. Microalgae are photoautotrophic microorganisms which primarily require carbon and energy. They need resources such as light, carbon dioxide, air, nutrients and proper growing conditions like optimum temperature and pH. Biomass produced from the microalgae can be used for biofuel

production, lipids or fatty acids, animal feeds, chemical substances, and many more products. Currently, microalgae is commercially cultivated for the high-value pharmaceutical products. However, the large-scale biofuel production from microalgae is not economical and sustainable due to high production cost and technological limitations.

Microalgae can either be cultivated in an open-pond system or in a closed system. In this work, microalgae cultivation in a controlled environment closed system is the main focus. A *photobioreactor* is a closed system used for cultivation of microalgae. Unlike open system, photobioreactor controls the supply of carbon and energy, and achieves the monoculture cultivation.

The main factors in the cultivation of microalgae in a photobioreactor are gas exchange (CO_2 and O_2) in and out of the PBR, sufficient light supply and distribution, balanced nutrients in the growth medium, proper mixing of the medium, and prevention of secondary metabolites accumulation in the PBR (Lee & Paisson, High-Density Algal Photobioreactors using Light-Emitting Diodes, 1994). Of all, controlling light delivery and distribution are the greatest challenge.

The major problem in the photobioreactor system is inefficient light penetration/utilization. Light that enters the photobioreactor is generally absorbed by the microalgal cells in the medium. At the same time, light is also scattered by the microalgal cells, dissolved nutrients and gas bubble flumes. To improve the light utilization in the system, light behavior with other factors of the photobioreactor are studied. A subsequent chapter will deal with the method to redistribute the light in the photobioreactor to achieve better light utilization.

This thesis work explores the light behavior in the flat-plate photobioreactor system. It presents the factors that affect light behavior in the system. It demonstrates the interaction of light with different factors of a photobioreactor system such as gas bubble flumes, biomass concentration and light path length.

Light is the primary energy source for any photosynthetic microorganisms. The metabolic activity of microorganisms is largely driven by the solar energy. Since microalgae are photoautotrophic microorganisms, they require light energy within the PAR range, which is from 400 to 700 nm, to initiate photosynthesis. In addition, they use water as the electron source and CO_2 gas as the carbon source.

The purpose of the illumination in a photobioreactor system is to provide light to all cells initiating photosynthesis. Light availability to cells is limited due to many factors like biomass concentration in the medium, PBR light path length and incident light intensity. These factors largely affect the light penetration in the system. It leads to the occurrence of *mutual shading* in the culture medium.

The ‘mutual shading’ is the most common problem in the photobioreactor. It creates no or low lit zone in the culture medium. This happens when cells in the lit zone block the light from reaching the cells in the dark zone (Lee 1999). The cells that present away from the illumination source don’t get sufficient light to initiate photosynthesis. The easiest way to resolve this problem is to use excessive light energy which may enhance the deep light penetration into the medium. However, excess light may cause over-heating and photo-inhibition to the cells in the lit zone.

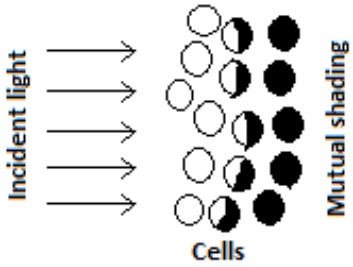

Figure 1.1. Mutual shading of algal cells (Carvalho, et al. 2011)

Mutual shading affects the production of biomass by limiting light availability to cells in the reactor. It is the phenomenon that happens when cells close to the illuminated surface absorb more light than required which leads to a shortage of light available to cells behind them. Dark zones are developed in the photobioreactor where cells are not able to get sufficient light for growth. A depiction of mutual shading is shown in the figure 1.1.

This thesis work also explores the concept of light guides which can be used to improve the light transmission into the high density PBR system. Different types of light guides are designed, tested and analyzed.

The technique of light transmission using light guides is explored. A light guide is an optical material used to transfer light rays from the source to the target using multiple internal reflections. It is otherwise called light pipe or waveguide. The concept of guided light was also introduced in the photobioreactor as part of its illumination system. Some related work has previously been done with the light guides in a photobioreactor system (Whithead, et al. 1982). Light guides can be used in the photobioreactor to reduce the dark zones in the system.

The light guide is used to collect light flux from the source on its dielectric surface and uses total internal reflection (TIR) to propagate light through it delivering it at the other end to the target. The focus is mainly on the design of different types of light guides. Light guides can be designed based on different geometrical shapes. Light guides can be made in any form or shape such as cylindrical, rectangular or conical (Gupta, et al. 2001). Cylindrical light guides (rods) are taken for this study. Different types of light guides are made out of the basic cylindrical shape. Design attributes are the diameter of the guide, the length of the guide and the exit surface angle of the guide. The light guides are tested and analyzed for their optical behavior such as photon transmission efficiency, which is greatly affected by the surface finish, volume scattering, and optical geometry.

Light guides can also be used to split the light source. For example, light from a single light source can be transmitted through the light guide and can transmit light out of the light guide at multiple output locations along the path of the guide. This can be achieved by reducing the diameter of a guide at each output surface along the path of light propagation in the guide. Light guides can also distribute the light uniformly at the output surface. However, the uniformity of light distribution completely depends on the light guide geometry and the input light distribution.

Light guides can be used in a flat-plate photobioreactor as part of the light transmission system. It can be a possible solution to solving the light penetration problem in a high density culture grown in a flat-plate photobioreactor (PBR) system. By employing light guides in the system, light can easily be transmitted into the high density culture to light the dark zones of the reactor which results in high photon usage by the photosynthetic organism in the reactor.

The objectives are:

1. Determine the interaction of incident light radiation with the gas bubbles, biomass and light path length.
2. Develop equations that relate the three factors
3. Determine the extincition coefficient of light path length, biomass concentration and gas bubbles.
4. Design the light guides with different design factors such as diameter, length, angle of exit surface and number of sections
5. Determine the photon transmission efficiency of the light guides.

2. LITERATURE REVIEW

2.1. Photo-autotrophic microorganisms

Microalgae are photoautotrophic microorganisms, which require carbon and energy source in the form of CO_2 and light respectively. Photoautotrophic microalgae that use light, carbon dioxide, inorganic nutrients and water will produce algal biomass through photosynthesis (Chisti 2007). The biomass can further be converted into many useful products such as saturated fatty acids or lipids, starch and glycogen. The process of photosynthesis in the photoautotrophic organisms is initiated by the light radiation in the visible region of an electromagnetic radiation spectrum.

2.2. Mass production of microalgae

Microalgae can be cultivated in two ways, open pond system and closed photobioreactor system. Microalgae use light from the natural sunlight, assimilate nutrients from the medium and carbon dioxide from the air. Light is the limiting factor in both systems (Pulz and Scheibenbogen 1998). Raceway ponds are used for large-scale commercial biomass cultivation. Each system has its own advantages and disadvantages over the other one as discussed in table 2.1 (J. U. Grobbelaar, 2009).

2.3. Photobioreactors

Photobioreactors are a closed system with controlled environment for algal growth. Unlike open pond system, the supply of required resources such as light, CO_2 and O_2, nutrients, minerals and water are provided in a control manner to the algal cells. There are different types of photobioreactors available for algal cultivation. Tubular and

flat plate-type photobioreactors are commonly used (Qiang and Richmond 1996). Comparatively plate-type photobioreactors have more illumination surface than tubular photobioreactors. The optimal temperature and pH, dissolved CO_2, inorganic nutrients, water and light are the requirements of algae for good yield of biomass. All these growth factors can be controlled in closed system photobioreactors.

Table 2.1. Advantages and disadvantages of closed and open algal cultivation systems.

Parameters	**Open ponds (raceway ponds)**	**Closed systems (PBR)**
Contamination risk	High	Low
Water losses	High	Low
CO_2 losses	High	Almost none
Reproducibility of production	Variant but consistent over time	Possible within certain tolerances
Process control	Complicated	Less complicated
Standardization	Difficult	Possible
Weather dependence	High	Less because protected
Maintenance	Easy	Difficult
Construction costs	Low	High
Biomass concentrations at harvesting	Low	High
Overheating problems	Low	High
Super dissolved oxygen concentrations	Low	High

The design parameters in the photobioreactor system are gas exchange in and out of the reactor, light supply and distribution, maintenance of components of nutrient medium, and prevention of accumulation of secondary metabolites (Lee & Palsson, High-density algal photobioreactors using light-emitting diodes, 1994).

2.4. Mixing of biomass and nutrient medium

Mixing is required in the photobioreactor system to move the cells between the photic and dark zones in order to get enough light energy for all the cells. It eventually increase the overall light utilization in the PBR system.

The primary objective of mixing the medium is to move the cells between photic and dark zones in order to expose the cells to get light energy for their photosynthesis process. Mixing helps to avoid cells deposit at the bottom of the enclosed chamber which keeps cells unfloculated. It also helps to keep the cells in suspension, eliminate heat, help nutrient distribution, and improve gas exchange (Lee & Palsson, High-density algal photobioreactors using light-emitting diodes, 1994). It creates turbulence which improves the fluctuating light regimes in the medium and enhances the mass transfer between medium and organism (Grobbelaar 1994).

Qiang and Richmond (1996) reported that minimum mixing rate required to prevent microalgal cells from wall growth and settling of biomass is 0.6 liters per liters of culture per minute (L L^{-1} min^{-1}).

Microalgal cell can be damaged by turbulent mixing or by physical or bubble burst. Cell are subjected to high hydrodynamic stress, which results in low biomass productivity (Gudin and Chaumont 1991). The results of over mixing are cell filament breakdown, development of foam in the PBR system, and leaky cells (Qiang and Richmond 1996)

Mixing can be done by mechanical means like stirring or air bubbles sparging. Lee and Palsson (1994) reported that the sparging will increase the light penetration

depth with the help of exitence of air bubbless and will induce mixing through bubble rise. Leppinen (2001) and Shamoun, et al. (1999) reported that the light attenuates with the concentration of gas bubbles.

2.5. Extinction coefficient

Equation 2.1 shows light attenuation with the biomass concentration. The light is passed through the distance (l) in the solution of known concentration. The initial light intensity (I_0) and the final light intensity (I_x) are measured. The extinction coefficient can be calculated using equation 2.2 (Clayton 1970)

$$I_x = I_0 e^{-a_c C l} \tag{2.1}$$

$$ln\frac{I_0}{I_x} = a_c C l \tag{2.2}$$

Where, a_c= extinction coefficient

C = Concentration, kg/m^{-3}

l = optical depth, mm

$$Extinction\ coefficient\ of\ the\ biomass, a_c = \frac{\ln\left(\frac{I_x}{I_o}\right)}{C_b l}\ , \text{m}^2/\text{g} \tag{2.3}$$

$$Extinction\ coefficient\ for\ light\ path\ lengh, a_c = \frac{\ln\left(\frac{I_x}{I_o}\right)}{l}, \text{m}^{-1} \tag{2.4}$$

$$Extinction\ coefficient\ for\ the\ bubbles, a_c = \frac{\ln\left(\frac{I_x}{I_o}\right)}{l}, \text{min/m}^4 \tag{2.5}$$

Equations 2.3, 2.4 and 2.5 are used to determine the extinction coefficients for biomass, light path length/depth and bubbles respectively.

2.6. Nature of light

Light is fundamentally a part of an electromagnetic radiation. Visible light is the part of electromagnetic radiation spectrum which falls in the waveband of 400 – 700 nm. Light has dual behavior as waves and particles. As a charged particles, light carries energy in the form of discrete frequencies or packets, known as *quanta*. These massless particles have momentum are also called *photons* (Falkowski and Raven 1997). It is the term coined by a chemist, GN Lewis, in 1926.

The following equation shows that the energy (ε) of a photon is directly proportional to the frequency (ν) of the radiating wave. The proportionality factor is called Plank's constant (h).

$$\varepsilon = \mathrm{h}\nu \tag{2.6}$$

Where, $\mathrm{h} = 6.625 \times 10^{-34}\ Js$

In an other relation, the energy (ε) of the photon is inversely proportion to its wavelength (λ). It is expressed as follows

$$\varepsilon = \frac{\mathrm{h}c}{\lambda} \tag{2.7}$$

This relation implies that the shorter the wavelength, the greater the photon energy. The energy of 1 eV is carried by a photon at 1240nm (infrared region). Therefore, the energy at any wavelength (ε_λ) can be calculated by following equation.

$$\varepsilon_\lambda = \frac{1240}{\lambda} \tag{2.8}$$

2.6.1. Photosynthetic active radiation (PAR)

Photosynthetic active radiation (PAR) is defined as the electromagnetic spectrum of waveband from 350 to 700nm, which is the visible light spectrum that is absorbed by the photosynthetic microorganisms to initiate the of light reaction processes of photosynthesis. The shorter wavelength radiation below 350nm have more energy and can damage the photosynthetic cells, while the longer wavelength radiation has less energy which is not enough to initiate the photosynthesis process.

Chlorophyll in the chloroplast of the organism is more sensitive towards the blue and red region of the visible light spectrum. While the human eye is more sensitive towards yellow region of the visible light spectrum. Figure 2.1 shows the response of human eye and photosynthetic organism towards visible light.

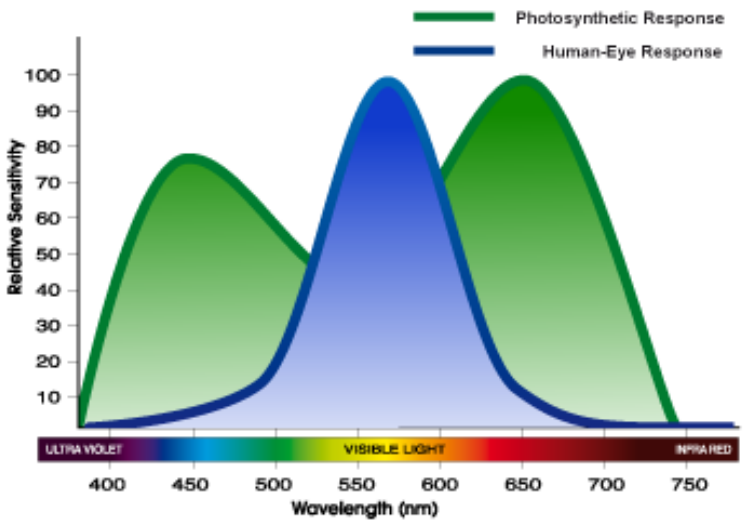

Figure 2.1. Chlorophyll and human eye response.

The energy from visible light spectrum can activate the photosynthetic process of microalgae. Equation 2.7 suggests that energy is inversely proportional to wavelength. In the visible light spectrum, red light has less energy than blue light.

Since photosynthesis is a quantum process, the concept of photosynthetic photon flux (area) density (PPFD) is commonly used for light measurements. The unit of PPFD is μmol $m^{-2}s^{-1}$.

2.7. Photosynthesis

Photosynthesis is the process of converting light energy into useful chemical energy such as ATP and NADP. Photosynthesis involves three basic processes which are light absorption, energy transfer and primary charge separation. These processes are called as light reactions of photosynthesis (Falkowski and Raven 1997). Rubio, et al. (2003) proposed that there are two steps involved in the photosynthesis in the microalgae. They are fast photochemical reaction and slow enzyme-controlled reaction.

All photosynthetic organisms have light harvesting chlorophyll (LHC) pigments such as chlorophyll a, chlorophyll b, and chlorophyll c. The light reaction center is the place where the absorbed light energy will be converted to photochemical energy. The photosynthetic process can be divided into two parts as light reactions and dark reactions. There is also a gas exchange between media and organisms.

2.7.1 Light reactions

Light reactions mainly take place in the chloroplast of the cell. Light energy is absorbed by the light harvesting chlorophyll pigments (LHC). In light reactions, NADP is reduced to $NADPH_2$ (light reaction 1) and oxygen is evolved from water (light

reaction-2) as shown in figure 2.2. These processes took place in two corresponding light reaction systems called photosystem I and photosystem II. In microalgae, the absorbed light energy can be transferred to photosystem I or photosystem II or both (Kirk 1994).

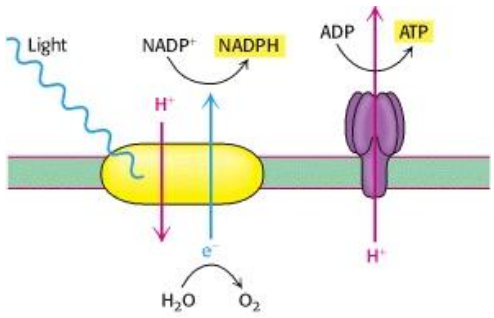

Figure 2.2. Light reaction of photosynthesis (Berg, Tymoczko and Stryer 2002).

The absorption spectrum of chlorophyll pigments in the organism is shown in the figure 2.3.

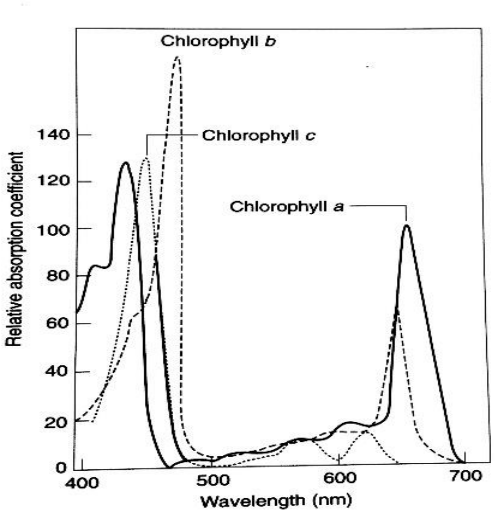

Figure 2.3. Absorption spectrum of light harvesting cholorophyll pigments (Falkowski and Raven 1997).

2.7.2 Dark reactions

Carbon dioxide is used in the dark reacions of photosynthesis (Nielsen 1966). In dark reactions, CO_2 is reduced to carbohydrates, primarily sucrose and startch, by using $NADPH_2$ from the light reactions. Energy from the light reaction was used to breakdown the ATP to ADP. This reaction is also known as the *Calvin cycle* or *cellular respiration*.

The overall photosynthetic process can be expressed in the following equation as

$$CO_2 + 2H_2O \xrightarrow{\sim 8h\nu} (CH_2O) + H_2O + O_2 \quad (2.9)$$

It shows that light and carbon dioxide are used in the process of photosynthesis which results in production of biomass and evolution of oxygen. According to the z-scheme, the minimum photon requirement to initiate the photosynthesis is *8 mol photons* which are required to produce 1 mol of oxygen (Osborne and Geider 1987). The energy from one mole of 680 nm photons is equivalent to about 50W (Lee & Palsson, High-density algal photobioreactors using light-emitting diodes, 1994).

2.8. Photosynthesis-Irradiance curve

2.8.1 Light compensation point

Photosynthetic and irradiance ($P - E_d$ curve) curve is extensively used to understand the response of algal photosynthesis to light intensity. Grobbelaar (2006) showed that there are three regions such as light-limited region, light-saturated region and photoinhibiton region.

$$P_E = E_a \phi_E \quad (2.10)$$

Where,

P_E = Photosynthetic rate at given irradiance E

E_a = Light absorbed by the organism (quanta m^{-2} sec^{-1})

ϕ_E = Quantum yield at irradiance E (Falkowski and Raven 1997)

To drive the photosynthesis in algae, the light energy is required to have sufficient intensity. When light is supplied to the algal cells, the intensity should reach the point where light energy can be used to drive photosynthesis in the algal cells. This point is called the light compensation point (I_c). The intensity below this point is not sufficient for photosynthesis, it leads to dark respiration where O_2 is consumed and CO_2 is evolved. This is also called *photorespiration*. During this phase, there is no cell growth. Above the compensation point, the region is called light region. (J. U. Grobbelaar 2009)

Light region can be further divided into three regions based on the intensity and growth response (figures 2.4 and 2.5). They are the light-limited region, light-saturated region and photoinhibition region. In light-limited region, the photosynthetic rate increases with the light intensity. While in the light-saturated region, the photosynthetic rate reaches maximum and becomes indepentant of the variation in light intensity. During this phase, the excess light energy will be dissipated as thermal/heat energy which affects cell growth (Yasushi 1991). It is otherwise called the photosaturation region. In the photoinhibition region, the cell growth and photosynthetic rate decrease with increase in light intensity. Sometimes, the excess light energy can damage the algal cells. (J. U. Grobbelaar 2009)

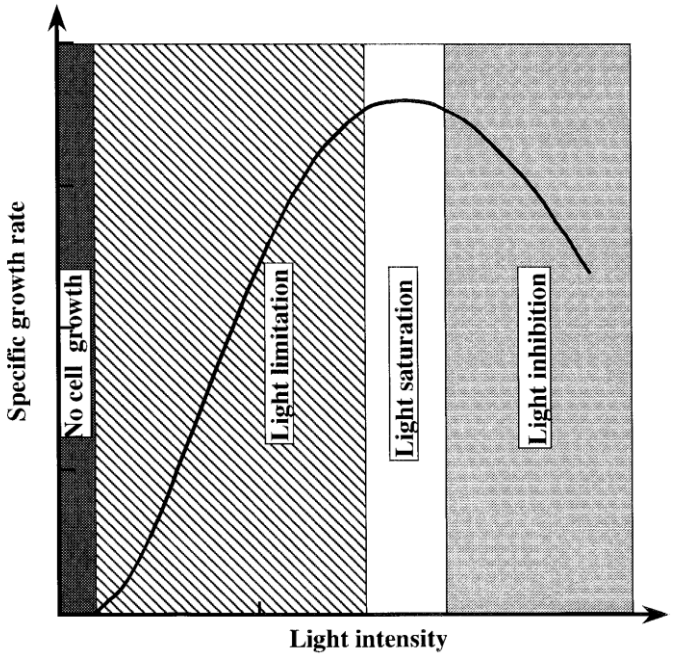

Figure 2.4. Effect of light intensity on specific growth rate of photosynthetic cells (Ogbonna & Tanaka 2000).

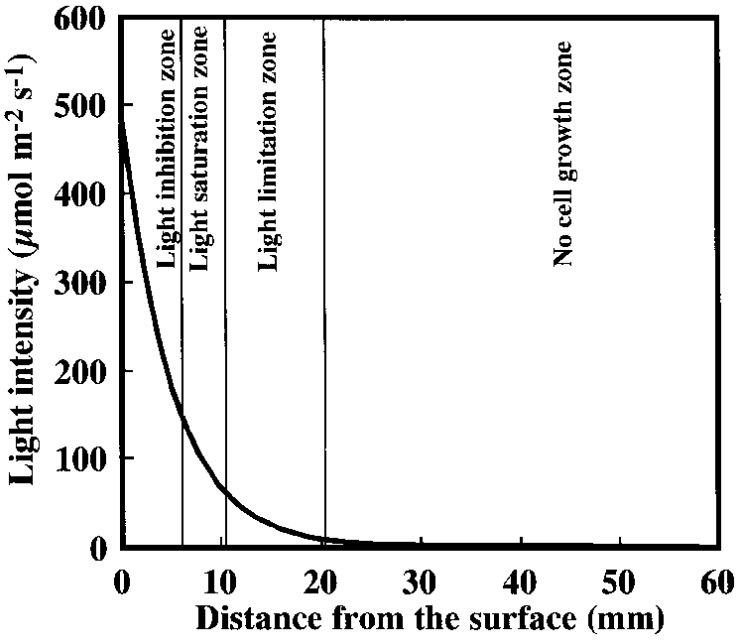

Figure 2.5. Light distribution inside a photobioreactor containing 1 g/L Euglena gracilis cells with a light absorption coefficient of 200 m^2 kg^{-1}. The photobioreactor was

illuminated from one surface at an intensity of 500 µmol m^2 s^{-1}. (Ogbonna & Tanaka 2000).

2.9. Effect of light on the microalgal cells

Microalgae have the tendency to absorb all light which they receive regardless of the intensity, frequency (continuous or intermittent) and wavelength in visible light region. Some times, these cells are affected by light.

Rubio, et al. (2003) reported that the photoinhibition is the result of light-induced damage to phosystem II, the repair mechanisms and the photoprotective process. This damage results in the inactivation of other systems in the process. The damaged cell take more than an hour to repair. Photoacclimation is the adaptation of cells that is exposed to high intensity after be in a low light intensity zone for a long period of time. It affects the cell growth.

2.10. Light sources

In an open pond system, the light source is the naturally available sunlight. The utilization of light in the open pond system is restricted by growing conditions. This results in low biomass productivity. Light is considered to be an important factor in biomass cultivation.

In photobioreactors, light sources are artificial lights such as tungsten lamp, fluorescent light, light emitting diodes (LED), etc. (Lee and Palsson 1994; Bula, et al. 1991). LEDs are white light or color specific lights such as red, green, and blue. Microalgae responsed differently with the spectral quality of light. Mostly, microalgae are sensitive towards red and blue lights.

Lee and Palsson (1994) reported that the use of LED light will minimize the photon loss, elimimate the heat generation by the light source, and filter the harmful wavelengths.

2.11. Light attenuation

When light enters the medium, it attenuates with depth. Light attenuates with the components of the medium, which are algal cells, nutrients, bubbles and other pigments (Grima, et al. 1999). Light is mostly absorbed and scattered by the algal cells, chemical substances and other particles in the medium (J. U. Grobbelaar 2009). Chlorophyll pigments are the light-absorbing pigments in the algal cell that absorb light for the photosynthetic process.

When light enters the photobioreactor, it attenuates exponentially while penetrating the cultural medium (Qiang et al. 1998). Light attenuation is a function of the concentration of algal cells and the light absorption of the chlorophyll pigments (Chrismadha and Borowitzka 1994).

At certain depth in the medium, the intensity of the incident light radiation drops below the light compensation point, which is called the *critical depth*. At this depth, the cultural medium is separated into two zones based on light availability. They are the photic zone and the dark zone. In the photic zone, the incident light radiation is available to all the algal cells. The algal cells have the tendency to absorb all the light, which falls on them regardless of the need for the photosynthetic process. This leads to mutual shading that commonly happens in a high-density algal culture. The algal cells near the illuminated surface blocks light from cells farther from illuminated surface. In the dark

zone, the incident light radiation falls below the compensation point that leads to photorespiration.

2.12. Light –dark cycles

Microalgal cells need both light and dark cycles for efficient growth and biomass production.

The issue of light attenuation and its effect becomes a big challenge. Researchers developed various method to improve the light-dark cycle of algal cells in photobioreactors. The most common method is intermittent flashing method (Park and Lee 2001). It is the method where high intensity light is given for a short period of time in regular intervals or intermittent flashing.

Lee and Palsson (1994) reported that even at higher light intensity, the PBR system will become light-limited eventually. Other method used to overcome mutual shading is to channel the light deep into the medium. This can be done by using optical fibers or light guides/ light pipes.

2.13. Theory of light guides

Light channeling devices are optic fibers, light guides, waveguides, light pipes, etc. Light guides are mostly used for internal illumination. Different types of lightguides/light pipes have been designed and tested (Gupta et al. (2001), Whithead et al. (1982)).

2.13.1. Ray tracing analysis

When a light ray (*i*) hits the dielectric interface of a light guide, it splits the incident ray into a reflected ray (*r*) and a refracted ray (*f*) due to the difference in the index of refraction of the mediums (n_1 and n_2) on each side of the interface.

When a light ray hits the interface at an angle normal to the surface, the ray exhibits reflection and refraction. The reflected ray travels in the opposite direction of the incident ray in the original medium with an angle which is equal to the incident angle (i.e. $\theta_i = \theta_r$). The refracted ray travels at a different angle in the other medium. The angle of the ray that hits the interface is called *the angle of incidence* (θ_i) and the angle of ray that travels in the other medium is called *angle of refraction* (θ_f). The angle of incidence and the angle of refraction can be calculated using Snell's law (Equation 2.11).

$$n_1 \sin\theta_i = n_2 \sin\theta_f \tag{2.11}$$

Where, n_1 = refractive index of medium 1, n_2 = refractive index of medium 2

As the light guide follows the law of reflection and refraction, the light ray refracts towards the normal when the light propagates from a low refractive index medium (n_1) to a high refractive index medium (n_2) whereas the light ray refracts away from the normal when light propagates from a high refractive index medium (n_2) to a low refractive index meduim (n_1) (figure 2.6).

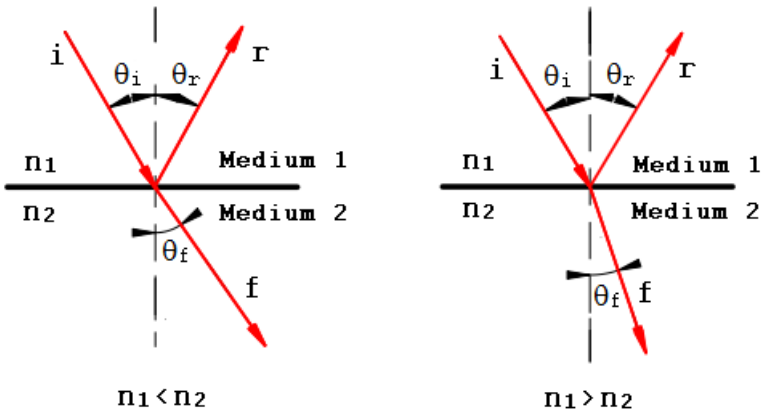

Figure 2.6. Travel of a light ray from one medium to other medium

The amount of light reflected and refracted can be calculated using Fresnel equations.

$$R = 100\% \times \left[0.5 \times \frac{tan^2(\theta_i - \theta_f)}{tan^2(\theta_i + \theta_f)} + 0.5 \times \frac{sin^2(\theta_i - \theta_f)}{sin^2(\theta_i + \theta_f)}\right] \quad (2.12)$$

Where, R = percentage of light that reflects from the surface

θ_i = the angle of incidence, degree; θ_f = the angle of refraction, degree

2.13.2. Total internal reflection

A light guide can exhibit an optical phenomenon called total internal reflection (TIR). Basically, a light guide has a front, side and exit surfaces as shown in figure 2.8. When an incident light ray (i) hits the entry surface (front) of the light guide, it refracts into the light guide due to the difference in the index of refractions of two mediums/materials. The refracted ray hits the internal side surface of the guide at a certain angle where some light can be refracted out of the light guide and some light can be reflected back into the light guide.

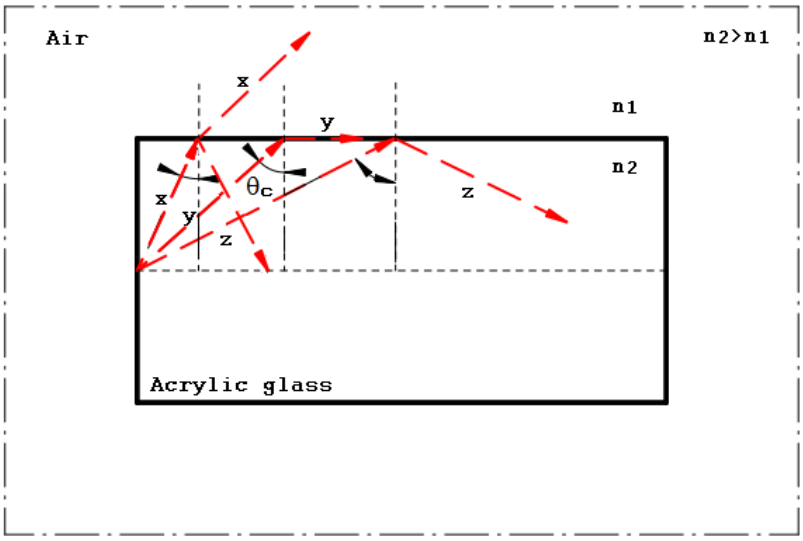

Figure 2.7. Total internal reflection

Figure 2.7 shows that the *light ray x* exhibits both refraction and reflection. *Light ray y* hits the side surface at the certain angle which makes the light refract along the surface of the light guide. The angle is called the *critical angle* (θ_c). If the angle of light hitting the surface is higher than the critical angle, then all light reflects back into the light guide which results in total internal reflection (TIR). *Light ray z* exhibits the phenomenon of *total internal reflection* (TIR). This phenomenon makes the light ray to propagate through the light guide towards the exit surface where light scatters out. Equation 2.13 can be used to find the critical angle.

$$\theta_c = \sin^{-1}\frac{n_2}{n_1} \tag{2.13}$$

Where, θ_c = the critical angle (deg); n_1 & n_2 = refractive index of the mediums

2.13.3. Acceptance angle

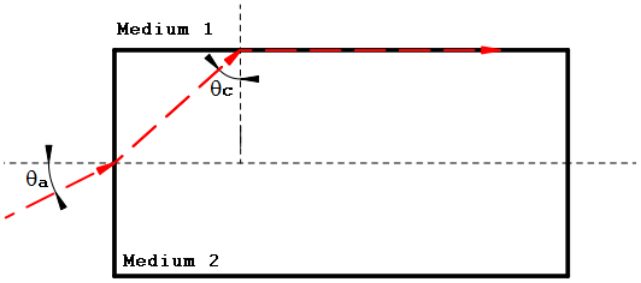

Figure 2.8. Acceptance angle

The acceptance angle is defined as the maximum angle of incidence at which all light exhibit total internal reflection in the light guide (figure 2.8). TIR can be calculated for a light guide using equation 2.15. Based on the calculation, the maximum acceptance angle (θ_{max}) of the guide is calculated to be 90°. This implies that all light that enters the guide undergoes total internal reflection. An internally reflected light ray will be emitted from the exit surface of the guide. The patterns of emitted light are affected by the shape and surface finish of the exit surface. The exit surface can either be flat or tapered. The tapered surface distributes the light in the form of Newtonian rings. The following equations are used to determine the acceptance angle of a light guide.

$$Numerical\ aperture\ (NA) = n_1 \times sin(\theta_{max}) = \sqrt{(n_2^2 - n_1^2)} \quad (2.14)$$

$$\theta_{max} = \sin^{-1} \frac{\sqrt{n_2^2 - n_1^2}}{n_1} \quad (2.15)$$

Where, θ_{max} = maximum acceptance angle

2.13.4. Ray propagation in a light guide

When a ray hits the air-acrylic interface of a light guide with an incident angle θ_1, it refracts into the light guide with a refracted angle θ_2 and reflects back with an angle θ_1. The refracted ray hits the internal side surface (acrylic- air interface) with an angle θ_3. By considering the angle θ_3 as the incident angle in the side surface, the ray exhibits both refraction and reflection again unless angle θ_3 is equal to or higher than the critical angle (θ_c). In that case, the ray exhibits only reflection from the side surface, which leads to multiple internal reflections along the guide's length. The propagated ray hits the output surface with an angle θ_4. Then it refracts out of the guide with an angle θ_5. In some cases, θ_1 and θ_4 are the same if the input and the output surfaces are parallel to each other. Figure 2.9 shows the ray propagation (red-dotted line) in a light guide from left to right end.

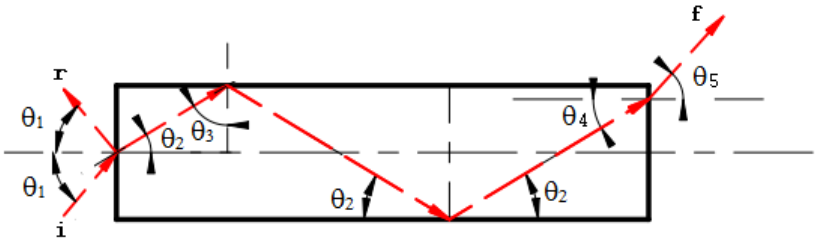

Figure 2.9. Ray propagation in a light guide

There are three types of rays involved in the propagation of light in a light guide. They are coupled rays, leaked rays and trapped rays.

a) *Coupled rays* are the rays that propagate through the light guide using total internal reflections and exit at the output surface on the other end. Most rays exit

the light guide but few rays are reflected back into the guide even from the output surface.

b) *Leaked rays* are rays that leak out of the side surface of the light guide. The rays that reflect back from the side surface reache the output surface with very little intensity.

c) T*rapped rays* are rays that are unable to refract out of the output surface due to TIR at all surfaces. More of the rays are reflected back from the output surface and they are trapped inside the light guide until that illumination from the source is stopped.

Due to volume scattering, surface imperfections and changes in light guide geometry, the coupled ray can be changed to a leaked or trapped ray.

2.13.5. Analysis of light guides

Since the refractive index of air and acrylic glass are known as 1.00 and 1.49 respectively, the critical angle (θ_c) and the maximum acceptance angle (θ_{max}) of the light guide can be calculated as 42.16° and 90° using the equations 2.13 and 2.15 respectively. Since the maximum acceptance angle is 90°, the incident angles at the flat input surface of the guide range from 0° to 90°. In this case, the corresponding refracted angles can be calculated as 0° to 42.16° using Snell's law (equation 2.13).

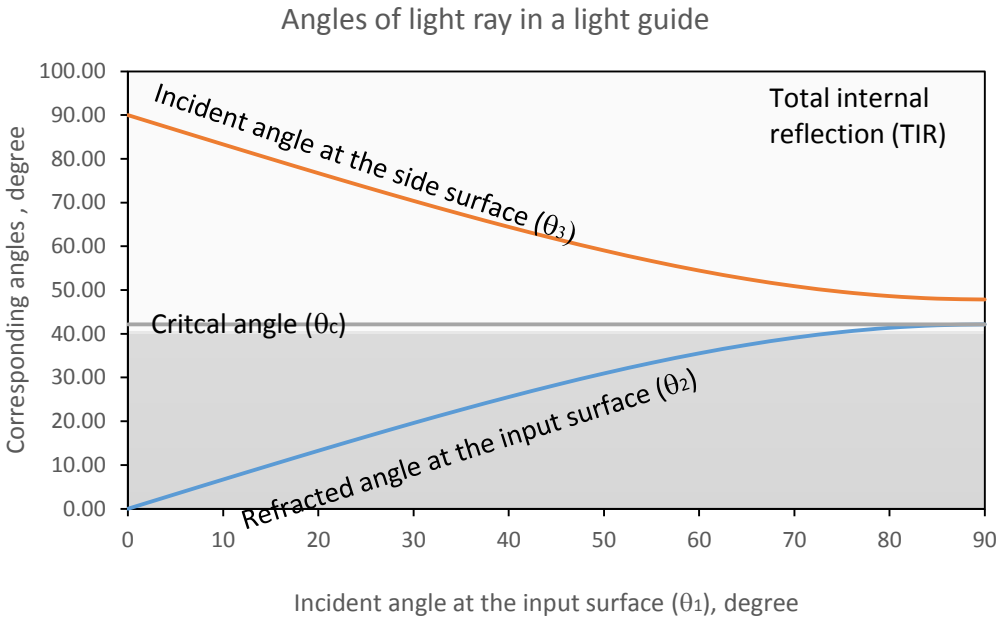

Figure 2.10. Angles of light rays in a light guide surrounded by air

All refracted rays hit the side surface, which is perpendicular to the input surface, with angles from 47.84° to 90°. Hence, the possible minimum angle of incident light at the side surface is 47.84°, which is higher than the critical angle (figure 2.10). Theoretically, this implies that all refracted light should undergo TIR.

When a ray undergoes reflection and refraction, a certain amount of light energy is lost. The percent of light energy lost by reflection can be calculated using Fresnel loss equation (equation 2.12).

Light guides are designed based on geometrical factors such as diameter, length and exit surface angle. The optical characteristics of light guides can be changed by varying each factor individually or in combination. Generally, the diameter and length factors do not influence the angle the rays are travelling in a light guide whereas the exit surface angle influences the angle of rays at the exit surface.

3. MATERIALS AND METHODS

3.1. Extinction Coefficient Test

Experiments were conducted to study the interaction of light with the factors of the flat-plate photobioreactor system and to determine the extinction coefficients for biomass, bubbles and depth. They are conducted in three phases. The first phase deals with the light interaction with gas bubbles in the medium; second phase deals with the light attenuation with the pathlength; and the third phase deals with the light interaction with the suspended biomass in the medium.

The light interaction with the factors of the PBR system are tested in laboratory experiment. Experiments are conducted to study the light interaction with biomass concentrations of 0 kg/m^3 to 1 kg/m^3; gas bubble rates of 0 liters/min to 10 liters/min; and pathlengths of 102 mm, 127 mm, 203 mm, 254 mm and 305 mm.

3.1.1. Materials used

A lab-scale *flat-plate photobioreactor* was used since it has a large illumination surface area that is best suited for this study. It was built with 9.5mm (3/8”) thick transparent plexi-glass. It is shaped like enclosed transparent box as shown in figure 3.1. Five different sized photobioreactors were built for the experiment. The size of these systems is 330mm (h) × 330mm (w) × l mm. The height (h) and width (w) remain the same but the length (l) of the system is varied. Lengths (l) are 101mm (4”), 152mm (6”), 203mm (8”), 254mm (10”) and 305mm (12”). These lengths (l) represent the light path length in the photobioreactor system.

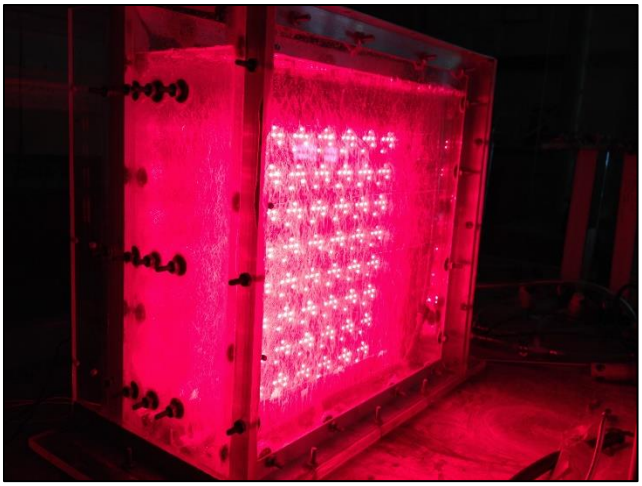

Figure 3.1. Flat-plate photobioreactor system.

A *LED light panel* 304mm x 304mm (12 x 12 inch) was used to illuminate the photobioreactor. Since the microalgae have a strong affinity towards 650 - 700nm wavelength light, red light with 656 nm wavelength is used in the experiment. The light panel is connected to the power supply which controls the voltage and the current supplied to the LED lights. A constant current and voltage (11.2V and 1.17A) were maintained for the experiment to keep the light intensity constant (Lee, 1999).

A *sparger* or a *diffuser* was placed at the bottom of the system to distribute the mixture of CO_2 and air into the medium. These gases help stir and mix up the medium in order to keep the microorganisms in suspension for better light, nutrient and gas utilization. The flow rate of air and CO_2 is controlled and monitored by an air flow meter (Model No: PMR2-01006 Cole Parmer Inc).

A *spectrometer* (Model no: USB4000 Ocean Optics Inc.) was used to measure the light intensities in the experiment. It has an optic sensor which collects the light and passes the light through an optic fiber to the spectrometer. The light intensity was monitored and recorded with the help of *SpectraSuite* software.

A *grid* was used to hold the optic sensor for the experiment trials. It ensures the placement of the optic sensor at the same given location in all tests. It is made up of plexi-glass which has an array of holes which are 51 mm apart from one another (figure 3.2). The light intensities are measured at 15 points on the illuminated exit surface of the PBR. The center point of the grid is designated as (0,0). The other points are designated with respect to the center of the grid such as (0,2) and (2,0) where the earlier represent the point which is 51mm from the center point in *y* direction and the latter represent the point which is 51mm from the center point in *x* direction.

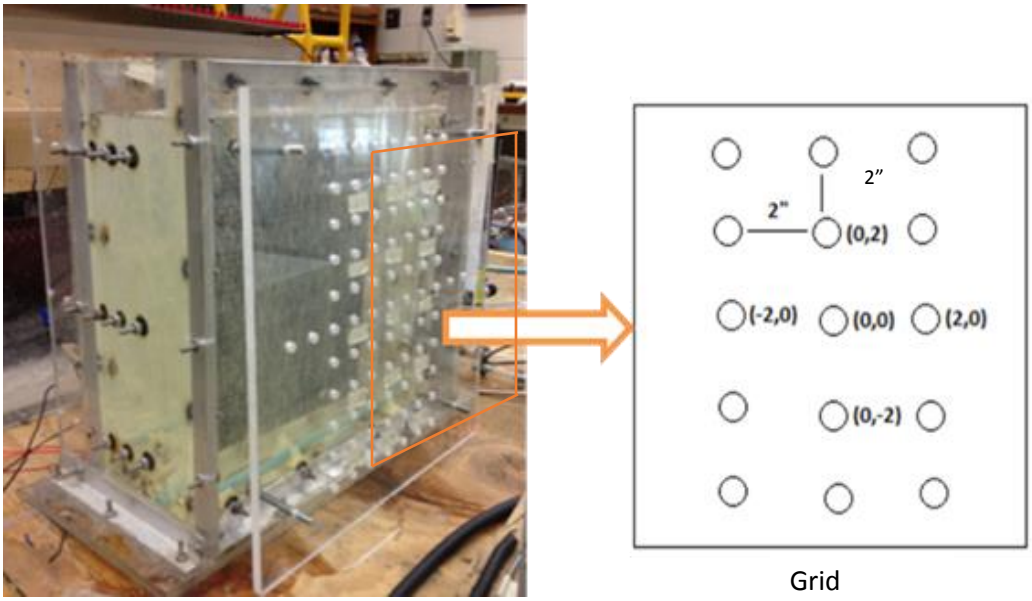

Grid

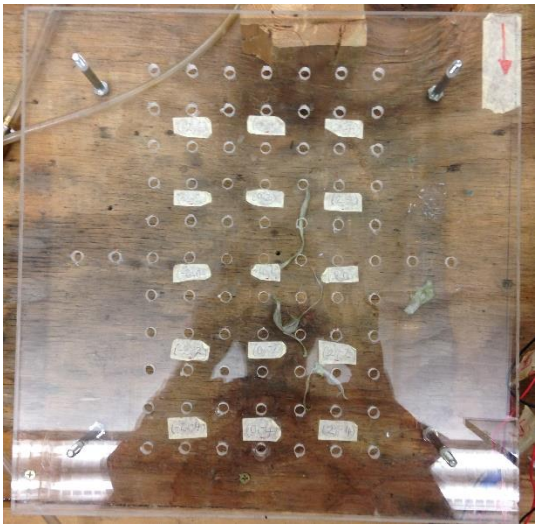

Figure 3.2. A schematic and original representation of a grid

A culture of *Chlorella vulgaris* was used in the experiment. *C.vulgaris* was grown in the medium of BG-11 which contains macro and micro nutrients. Figure 3.3 shows the complete setup of the light experiment.

3.1.2. Test Procedure

The experiment was conducted in three phases to study the light activity in the photobioreactor. The photobioreactor was illuminated on one side and the light is measured at the other side. The initial light intensity is kept constant for the first two phases of the experiment. The water generally was filled to ¾ of the PBR volume. A complete experimental setup is shown in the figure 3.3.

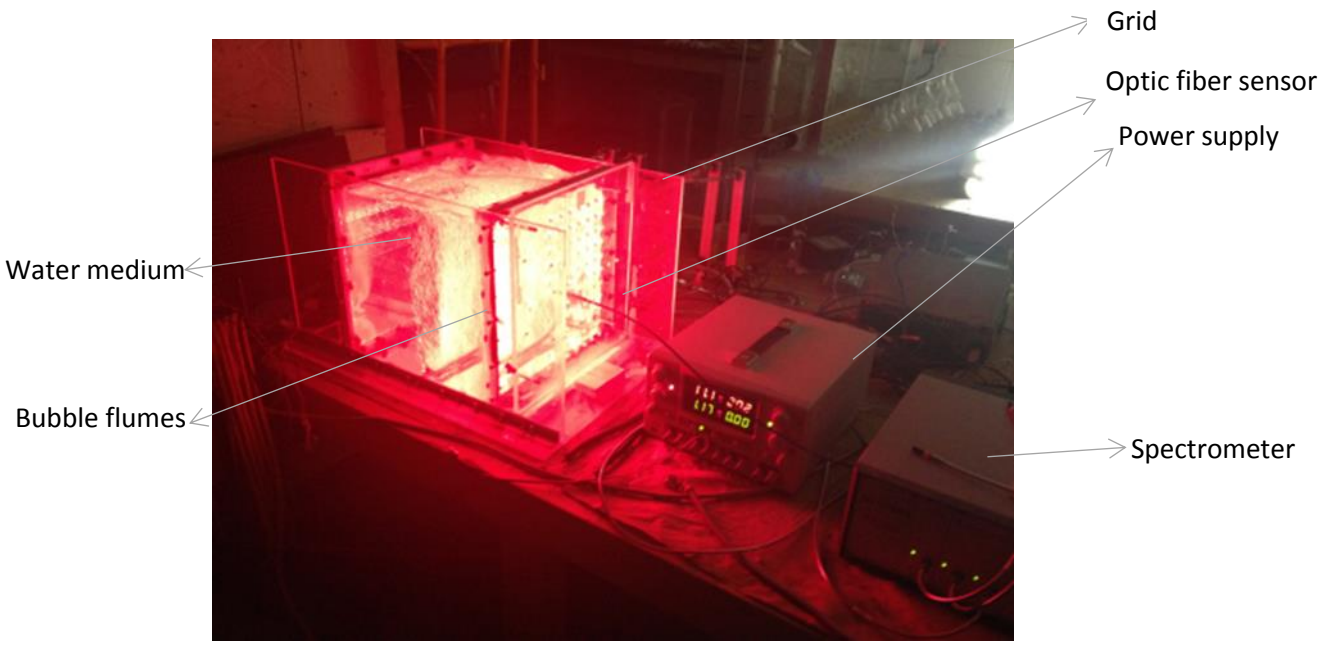

Figure 3.3. Photobioreactor light experiment setup

3.1.2.1. Phase 1: Light attenuation with distance

In this phase, the light is passed through the water medium in different sized photobioreactors. These photobioreactors have different light path lengths such as 101mm (4”), 152mm (6”), 203mm (8”), 254mm (10”) and 305mm (12”). This test helps study the light attenuation with distance.

3.1.2.2. Phase 2: Light interaction with gas bubbles

The light is passed through the system and is collected at the other side. When the light passes into the system it hits the medium and the gas bubbles which results in scattering of the light. The output irradiance is measured at 15 points on the exit illuminated surface using the grid and spectrometer. The mixture of air and CO_2 is supplied into the medium with different flow rates in the form of bubble flumes. The light activity is tested with different flow rates of gas bubbles which varies from 1 liter/min to 10 liters/min.

3.1.2.3. Phase 3: Light interaction with suspended biomass and dissolved nutrients

The same procedure of light supply and collection is repeated as in phase 1 and phase 2. The photobioreactor with dimensions of 330mm × 330mm × 101 mm is used in this phase. The light attenuation is monitored with different biomass concentration ranging from 0 kg/m^3 to 1 kg/m^3 with an interval of 0.1 kg/m^3. In all phases, the initial light intensity is the same.

3.2. Light guide test

An optical experiment system was developed to test and evaluate the light guides. The main purpose of the experiment was to measure the light output from the exit surface(s) of the light guide. The system is built in a way that the light flux loss should be minimized. It captures most of the light flux from the source and transmits it through the light guide. Figure 3.4 shows the complete experiment setup. The components of the system are:

1. LED Panel
2. Light channel
3. Compound lens system
4. Light guide holder
5. Integrating sphere
6. Spectrometer with optic fiber sensor
7. Light guide

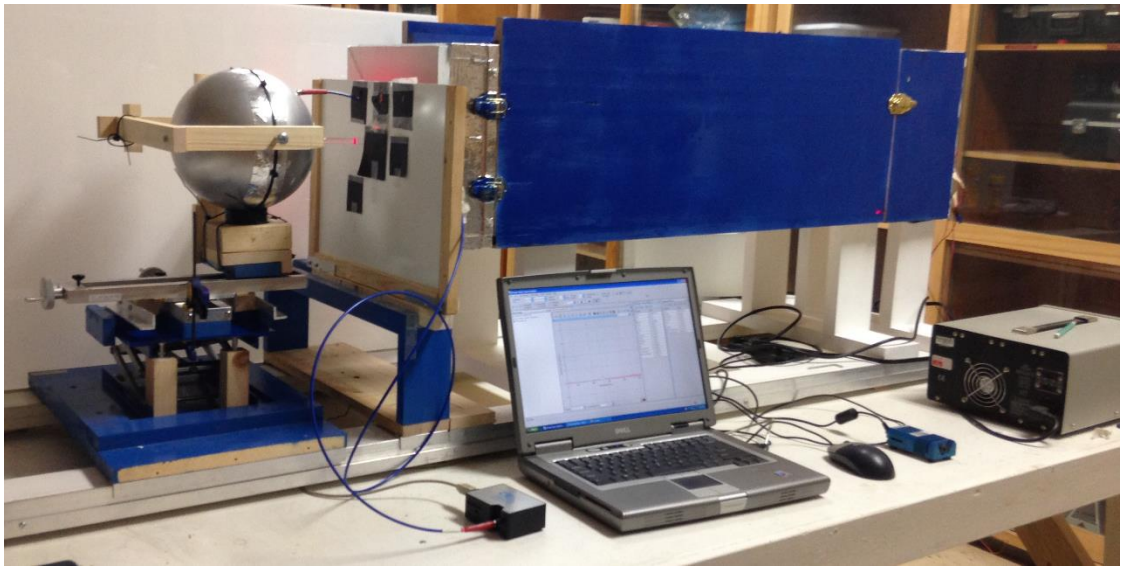

Figure 3.4. The experimental setup to test light guides.

3.2.1. Materials used

A LED panel with dimension of 264.16 mm × 264.16 mm (10.4”×10.4”) was used in the experiment. It has 64 pixels of LEDs. Each pixel contains red, blue and green LEDs. In each pixel, there are 6 red LEDs with peak wavelengths of 600 – 700 nm. Only red LEDs were used as a light source in the experiment. The LED panel is connected to a 3-channel power supply which controls the current and the voltage maintaining a constant initial light intensity throughout the experiment. The panel is placed on one end of the light channel box.

The light channel box is an enclosed box internally coated with high reflectance material such as barium sulfate. The barium sulfate coating guides the light from the LED panel to the lens system reducing the light flux loss. The length of the light channel box is 1.2 m.

A compound lens system consists of two Fresnel lenses of sizes 279.4 mm ×279.4 mm (11”x11”) and 127 mm×127 mm (5”x5”) placed 127 mm (5”) apart with a focal length of 177.8 mm (7”) and 127 mm (5”) respectively. The lens system converges the light to a focal point of 50.8 mm (2”) in diameter with the focal distance of 76.2 mm (3”). The angle of convergence is 26.56°. The light guide is placed at the focal distance from the lens system so that the converged light falls on the entry surface of the light guide. This system couples the light rays to the light guide surface.

The light guide was held by the *light guide holder* which is made up of cardboard with three holes of sizes 9.525 mm (3/8”), 25.4 mm (1”), and 50.8 mm (2”) that can hold all three diameters of light guides. The sizes of holes in the holder selected based on the light guide diameter. For instance, a 25.4 mm diameter light guide was placed in the 25.4mm diameter hole. The holes hold the light guides in alignment with the axis of the optical system. The holder can also be used to block the scattered light from the lens.

An *integrating sphere* with a diameter of 203.2 mm (8”) which is internally coated with high reflectance barium sulfate was used in the experiment. It collected the emitted light from the light guide. It was placed on a 3-axes adjustable unit which aligned the integrating sphere with the light guide. An optic fiber sensor was placed in the integrating sphere to measure the light intensity with the help of a spectrometer (OceanOptics, Inc). An integrating software (SpectraSuite, OceanOptics,Inc) was used to record the light intensities.

A *light guide* is made up of a solid plexiglass glass rod which has three basic surfaces. It has two end surfaces (input and output surfaces) separated by the length (L) and one side surface (perimeter of the guide) (Figure 3.5). When the light rays enter the

light guide at the dielectric interface, it propagates through the guide medium towards the other end where it escapes.

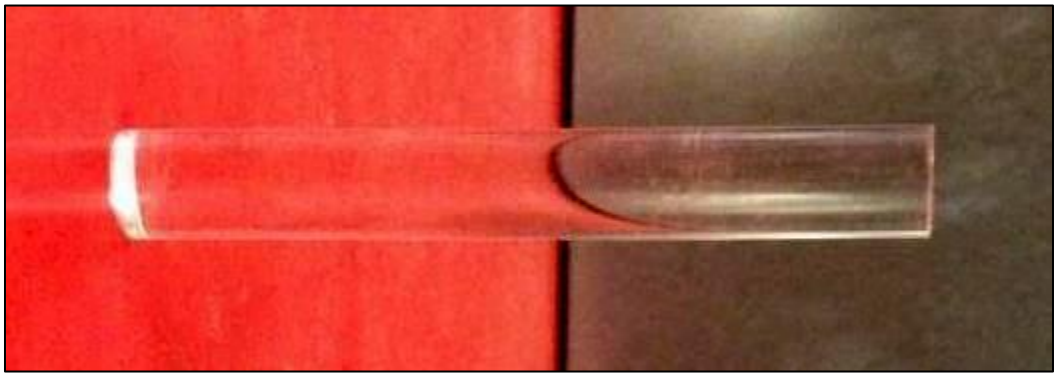

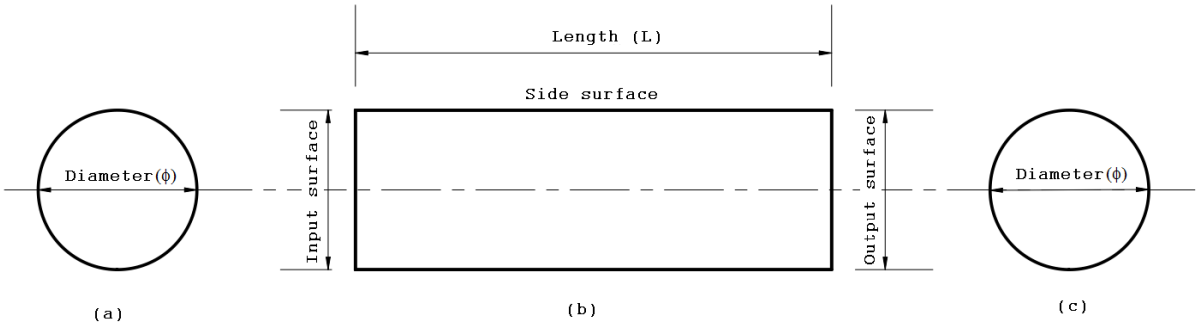

Figure 3.5. Schematic diagram of a light guide with (a) front view, (b) side view and (c) back view

The end surface where light enters is called an *input surface/entry surface*. The input surface is always flat, polished and smooth. The other end surface where light emits is called an *output surface*/*exit surface*. The exit surface can be made into either a flat or tapered end with angles like 30° and 60° to the axis of the guide. The change in the shape of the end surface of the light guide defines the light distribution pattern. All surfaces of the light guide are smooth and well polished.

3.2.1.1 Types of light guide

Light guides can be classified into two types based on the number of exit/output surfaces. They are simple and compound light guides.

Simple light guides are single-sectioned guides with one exit/output surface. Since single-sectioned light guides are cylindrical in shape, the diameter of the guide is equal along the length from input to output surface. Figure 3.6 shows the single-sectioned simple light guide with the length (*l*), the diameter (ϕ) and an exit surface angle (α).

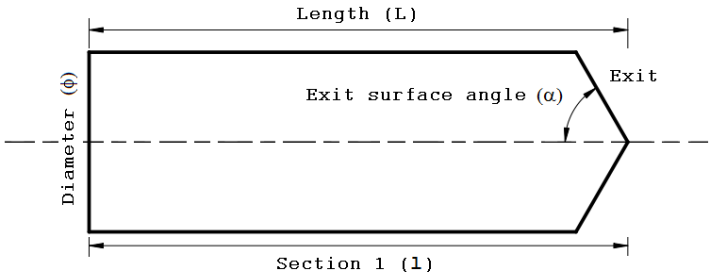

Figure 3.6. Single-sectioned simple light guide

Compound light guides are multiple-sectioned guides which are further categorized as a two-sectioned light guide or a three-sectioned light guide based on the number of exits/output surfaces. These light guides are primarily used to split the light from the source and delivering the light to multiple output surfaces.

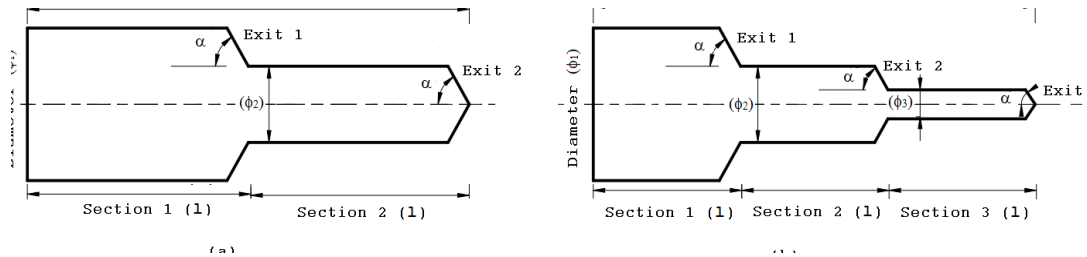

Figure 3.7. Schematic diagrams of multi-sectioned light guides: (a) a two-sectioned light guide and (b) a three-sectioned light guide

A compound light guide is divided by the number of sections which are equal in length (l) and the angle of the exit surfaces (α). However, each section of a light guide has different diameters. As shown in figure 3.7, two-sectioned light guides have two output surfaces (exit-1 and exit-2) and three-sectioned light guides have three output surfaces (exit-1, exit-2 and exit-3). With these multiple output surfaces, the light flux can be delivered at each exit surface of a compound light guide. The distribution pattern of the illumination and the amount of light energy released at each location are based on the geometry of the light guide, input light distribution and volume scattering. Figure 3.8 shows examples of the simple and compound light guides which are made out of acrylic glass rod.

Figure 3.8. Simple and compound light guides

3.2.1.2. Design factors

There are primary and secondary design factors. The primary design factors are diameter, length, and exit surface angle (taper). The secondary design factor is the number of sections/exit surfaces. Simple light guides have only primary design factors, whereas compound light guides have both primary and secondary design factors.

3.2.1.2.1. Primary design factors

Length (L): Light guides can be used to transmit light flux over short or long distances with minimal loss. Light guides with short lengths are more useful in the photobioreactor system. By considering this, short length light guides are taken for the experiment. To design the simple and compound light guides, three lengths of 101.6 mm (4”), 152.4 mm (6”) and 203.2 mm (8”) were used (figure 3.9).

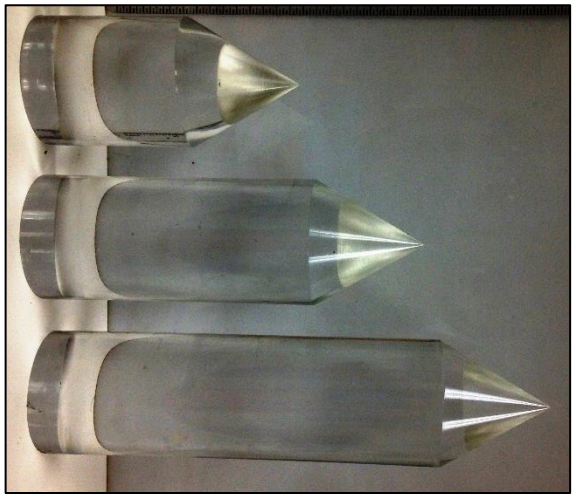

Figure 3.9. Light guides with different lengths (101.6 mm, 152.4 mm and 203.2 mm)

In a compound light guide, the lengths of the sections also needs to be considered. The sections are equally divided lengthwise in a compound light guide based on the number of exit surfaces. For example, a 101.6 mm (4”) long two-section light guide has

two exit surfaces which have equal length of 50.8 mm (2”). Similarly, 101.6 mm (4”) long three-section light guide is made with three exit surfaces of an equal 33.8mm (1.33”) length. The length of the section (l) in a compound light guide is calculated using equation 3.1.

$$Length\ of\ the\ section\ (l) = \frac{Length\ of\ the\ guide\ (L)}{Number\ of\ exit\ surfaces\ (N)} \quad (3.1)$$

***Diameter* (ϕ):** The diameter of the light guide is one of the important design factors. Since the diameter is directly related to the size of the guide, the surface area of input end increases with an increase in diameter. Three diameters (sizes) are considered for the experiment which were 9.525 mm (3/8”), 25.4 mm (1”), and 50.8 mm (2”).

Figure 3.10 shows the different sizes of simple light guides used. The simple light guide has single diameter. Since compound light guides have many sections, each section has different diameter (figure 3.10).

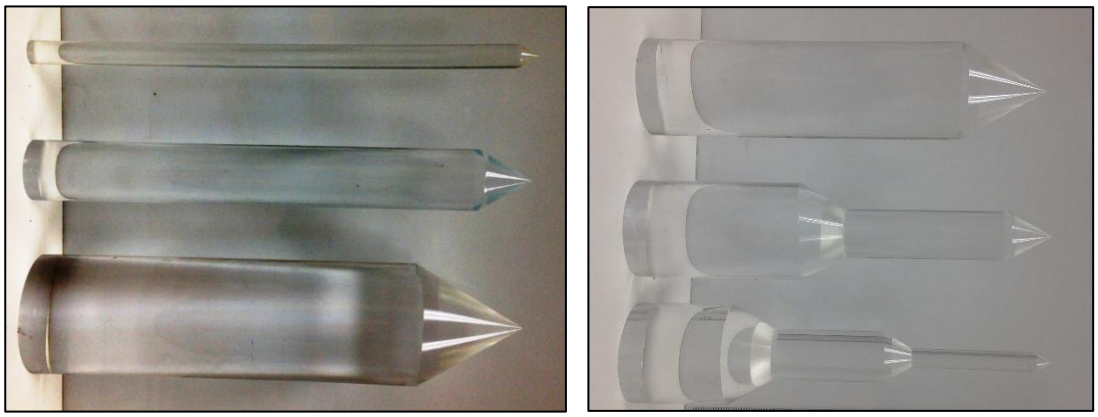

Figure 3.10. Light guides with different diameters (9.525 mm, 25.4 mm, and 50.8 mm)

***Exit surface angle (α)*:** The exit surface angle (taper) is an angle between the light guide exit surface and the optical axis of the light guide (figure 3.11*)*. It creates different light distribution patterns from the exit surface of the light guide. Exit surfaces can be made

into a flat or tapered surface. Three angles are considered in the light guide tests (figure 3.11) which are 30^0 (taper), 60^0 (taper) and 90^0 (flat). The angles of 30° and 60° make the exit surface into cone shaped surface that creates wide distribution patterns whereas the 90° surface is a flat surface that creates narrow distribution pattern. In a compound light guide, the angles of all exit surfaces were kept equal.

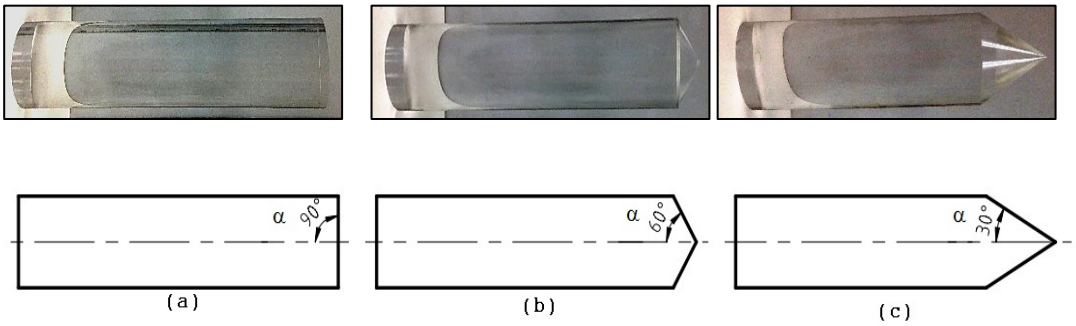

Figure 3.11. Light guides with different output surface, (a) Flat end with 90°; (b) taper end with 60° angle; and (c) taper end with 30° angle.

Table 3.1 shows the primary design factors and their variables (values). Many light guides of different geometric shapes can be made with the combinations of these design factors.

Table 3.1. Design factors for light guides.

Design factors	**Variables**
Length, L	101.6 mm, 152.4 mm, 203.2 mm (4”, 6”, 8”)
Diameter, ϕ	9.525 mm, 25.4 mm, 50.8 mm (3/8”, 1”, 2”)
Exit surface angle, α	30°, 60°, 90°

3.2.1.2.2. Secondary design factor

Number of sections (N): Number of sections is a secondary design factor which is considered exclusively for compound light guides. Compound light guides have two or more sections which each have a sectional length (l). The sections differ in diameter. For this experiment, two-section and three-section light guides are used.

With these design factors, 54 different light guides can be made (table 3.2). Among these, there are 27 simple light guides (type-I) and 27 compound light guides (type-II). In the compound light guides, there are 18 two-section and 9 three-section light guides. The sequence of sections in a compound light guide is arranged in a step-down manner from the input end. This means that the input end section has a greater diameter than the output end section. For example, two sequences can be made in two-section light guides which are 50.8 mm (2”) × 25.4 mm (1”) and 25.4 mm (1”) × 9.525 mm (3/8”). Likewise, one sequence of 50.8 mm (2”) × 25.4 mm (1”) × 9.525 mm (3/8”) can be made in three-section light guide. All these light guides are tested and evaluated for transmission efficiency.

Table 3.2. Light guides selected

No. of Section (N)	Exit slope angle (α)	Length of light guide								
		101.6 mm (4")			152.4 mm (6")			203.2 mm (8")		
		Diameter, (ϕ)			Diameter, (ϕ)			Diameter, (ϕ)		
		mm			*mm*			*mm*		
		50.80 (2")	25.40 (1")	9.53 (3/8")	50.80 (2")	25.40 (1")	9.53 (3/8")	50.80 (2")	25.40 (1")	9.53 (3/8")
One	90^0	×	×	×	×	×	×	×	×	×
	60^0	×	×	×	×	×	×	×	×	×
	30^0	×	×	×	×	×	×	×	×	×
		50.80 × 25.40 (2" × 1")		25.40 × 9.53 (1" × 3/8")	50.80 × 25.40 (2" × 1")		25.40 × 9.53 (1" × 3/8")	50.80 × 25.40 (2" × 1")		25.40 × 9.53 (1" × 3/8")
Two	90^0	×		×	×		×	×		×
	60^0	×		×	×		×	×		×
	30^0	×		×	×		×	×		×
		50.80 × 25.40 × 9.53 (2" × 1" × 3/8")			50.80 × 25.40 × 9.53 (2" × 1" × 3/8")			50.80 × 25.40 × 9.53 (2" × 1" × 3/8")		
Three	90^0	×			×			×		
	60^0	×			×			×		
	30^0	×			×			×		

***Note:** × denotes the light guides selected

3.2.2. Test Procedure

An experiment was conducted to test and evaluate the light guides for light transmission efficiency, which is defined as the percent of light transmitted through the light guide on a photon basis. It can be calculated by measuring input light intensity that enters the light guide and output light intensity that escapes out of the light guide.

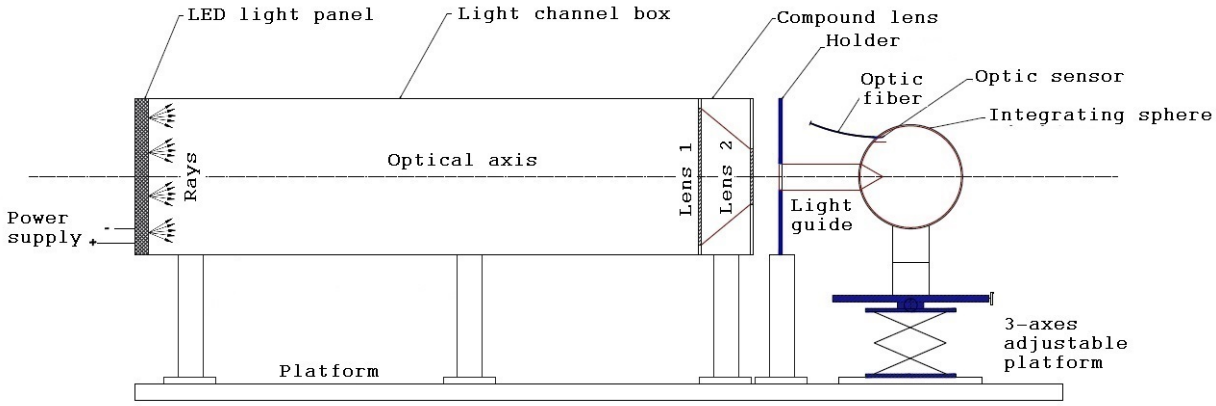

Figure 3.12. An optical experiment system to test light guides

As shown in figure 3.12, the direction of light rays is from the left end (source) to the right end (target) of the system. Rays from the source are guided through the light channel box and fall onto the compound lens system where rays converge on to the light guide input surface. The light guide propagates the converged rays from input surface to the output surface where they escape out of the light guide. The escaped rays are then collected by an integrating sphere and the intensity is measured with the help of spectrometer and optic fiber. Both simple and compound light guides can be tested in this system.

Firstly, all components of the system should be placed on a horizontal platform and be properly aligned with the optical axis of the system. As shown in figure 3.12, light rays from the light source are coupled with the light guide surface with the help of the light channel box and the compound lens system. The scattered light rays from the lens are blocked by the holder. Only converged rays are coupled with the light guide.

Secondly, the input light intensity is measured for all three sizes (diameters) of light guide. It can be measured by allowing the converged light rays to directly enters the integrating sphere.

Thirdly, the output light intensity is measured for all types of light guides. To measure the output light intensity, the output surface of the light guide should be inserted into the integrating sphere. A procedure was developed to get the light output measurement of side and exit surfaces. The measurement can be done by placing the light guide at different locations in the integrating sphere. For example, placing the integrating sphere at position 2 gives an output measurement of the exit surface whereas placing integrating sphere at position 1 gives output measurement of both sides and the exit surface. Figure 3.13 shows that the output of the side surface can be calculated by subtracting measurement 2 from measurement 1. Figure 3.13 shows the measurement locations for simple light guide.

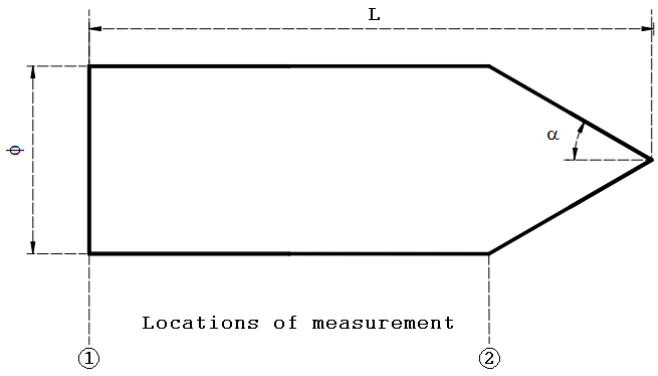

Figure 3.13. Simple light guide with measurement locations

A similar procedure is followed for output measurements for compound light guides. The output intensity of each exit surface is measured by placing the integrated

sphere at each exit surfaces. Figure 3.14 shows the placement of the light guide in an integrating sphere to measure light output at the exit surfaces.

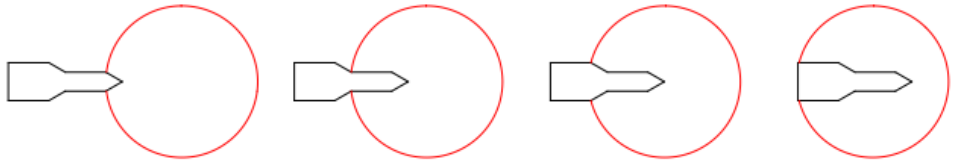

Figure 3.14. Placement of integrating sphere at different measurement positions for a two-sectioned compound light guide.

Based on the placement of light guides in the integrating sphere, there are 4 and 6 measurement locations for two- and three-sectioned light guides (figure 3.15). This allows for the output measurement of each side and exit surfaces of the compound light guides.

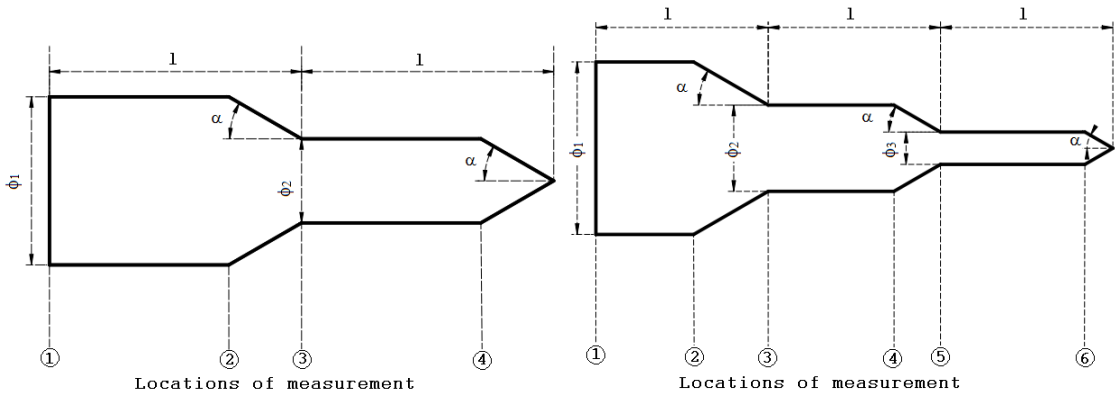

Figure 3.15. Compound light guides with measurement locations.

4. RESULTS AND DISCUSSION

4.1. Extinction coefficient

The results of phase 1 and phase 2 experiments are shown in table 4.1. The table shows the light intensity in different photobioreactors with different air flow rates. The results indicate the attenuation of light with an increase in the air flow rates in all photobioreactors.

The output irradiances are measured at 15 locations at the PBR exit side using the grid. Figure 4.1 shows the contour distribution of output light intensity at the exit side of a 152 mm PBR with no gas bubbles (Refer APPENDIX - D).

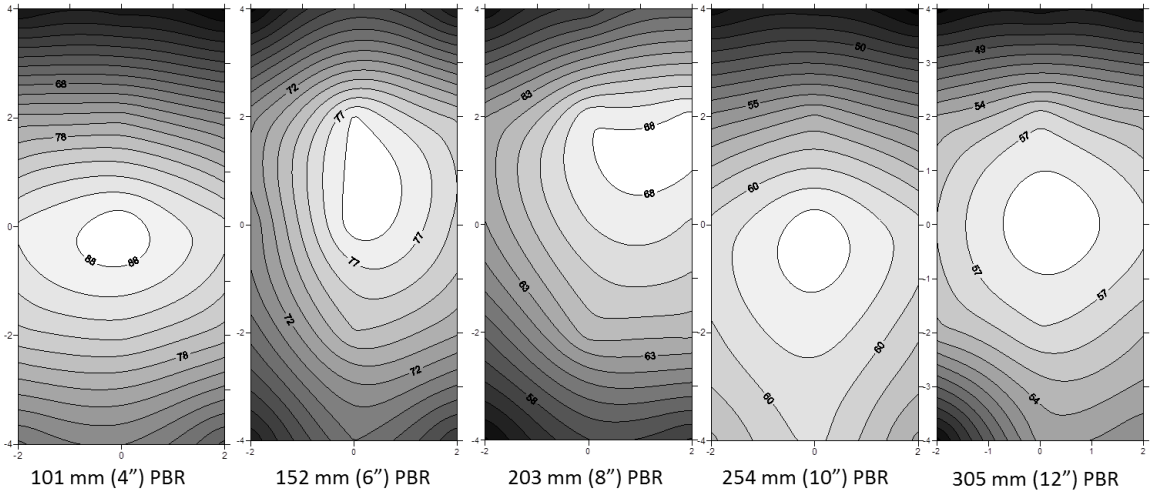

Figure 4.1. Contour representation of distribution of light flux at the exit side of the photobioreactor system

Figure 4.1 shows that the output light flux is high near the center region of the grid. The lowest flux was recorded near the corners of the photobioreactor. Thus, the intensity data measured at the center position were considered for further analysis.

Table 4.1 shows the output irradiance of light measured at the (0,0) position in the exit side of the photobioreactor system for different pathlengths and different flow rates of gas bubble flumes.

Table 4.1. Light intensity measurements for different air flow rates and different pathlength of photobioreactors

Light Intensity (μmol m^{-2} s^{-1}) at center position (0,0)					
	Depth of Photobioreactor (pathlength)				
Flow rate (liters/min)	**102mm (4")**	**127mm (6")**	**203mm (8")**	**254mm (10")**	**305mm (12")**
0	89.53	78.56	66.97	62.66	58.66
1	83.23	77.18	63.30	53.13	52.38
2	75.52	72.67	59.63	52.40	48.74
3	72.00	70.07	58.01	51.21	47.60
4	68.44	67.49	57.65	50.14	46.68
5	67.03	64.46	53.52	49.19	45.81
6	61.24	62.37	55.13	49.16	40.95
7	64.13	60.33	53.88	48.73	42.00
8	60.10	57.64	50.83	48.87	40.95
9	60.23	56.02	51.69	48.11	39.28
10	56.62	54.24	50.34	48.99	39.58

The incident light flux enters the PBR interact with the medium which attenuate the light along the pathlengths. Additionally, the light interact with the bubble flumes which is used for mixing the medium. Table 4.1 shows the output radiances measured at

the exit surface of the PBR with different pathlengths and different gas bubbles flow rates. These values are used for further analysis of extinction coefficients.

It can be seen that when the light flux passes through the medium, it attenuates from 106.33 μmol m^{-2} s^{-1} to 89.53 μmol m^{-2} s^{-1} in the 102 mm pathlength PBR. The light flux further drops down to 83.23 μmol m^{-2} s^{-1} with the introduction of gas bubbles into the medium at the flow rate of 1 l/min. The drop increases with an increase in the flow rates of gas bubbles in the medium.

It is found that there is a 7% drop in output irradiance due to the introduction of gas bubbles into the medium with 1 l/min flow rate (table 4.2). It implies that light attenuates when it interacts with the gas bubble flumes. The input irradiance of phase 1 and phase 2 experiments is measured as 106.33 μmol m^{-2} s^{-1}.

It also shows the light attenuation percentage across the different pathlengths and different gas flow rates.

4.1.1. Phase 1: Light attenuation with pathlength

Figure 4.2 shows the attenuation of light with distance/ path length of the photobioreactor. The light path length is the distance between the illumination source and the target. From the table 4.1, it can be seen that the light attenuates with the increase in the distance between source and target. The incident light intensity is 106.33 μmol m^{-2} s^{-1}. At 0 liter/min air flow rate, the output light flux decreases from 89.53 to 58.66 μmol m^{-2} s^{-1} across the photobioreactors which results in 34% light attenuation. Likewise, the total

light attenuation percentage across different photobioreactors (102 mm to 305 mm) at each air flow rate (0 l/min to 10 l/min) ranges from 30% to 37%.

The light attenuation is calculated by using the input irradiance and the output irradiance.

$$Light\ attenuation, \% = \frac{Output\ irradiance,\ \mu mol\ m^{-2}\ s^{-1}}{Input\ irradiance,\ \mu mol\ m^{-2}\ s^{-1}} \times 100\ \% \quad (4.1)$$

Table 4.2. Light attenuation across different pathlength of PBR with no gas bubbles

Path length, mm	Output light intensity, μmol m^{-2} s^{-1}	Light attenuation, %	Extinction Coefficient, mm^{-1}
102	89.53	15.80	0.002
152	78.56	26.12	0.002
203	66.97	37.02	0.002
254	62.66	41.07	0.002
305	58.66	44.83	0.002

The extinction coefficient of pure water at wavelength of 655nm is 0.371 m^{-1} based on the data of Pope and Fry (1997). The extinction coefficent is calculated with the test data using equation 2.4. It is found to be 0.002 mm^{-1} with the monochromatic red light peaks at 656 nm which is used in this experiment.

The equation developed from the test data is:

$$Output\ Irradiance,\ I_x = 108.8\ (\mu mol\ m^{-2} s^{-1})\ e^{-0.002\ x\ (depth,\ mm)} \quad (4.2)$$

Where, x = Light pathlength, mm

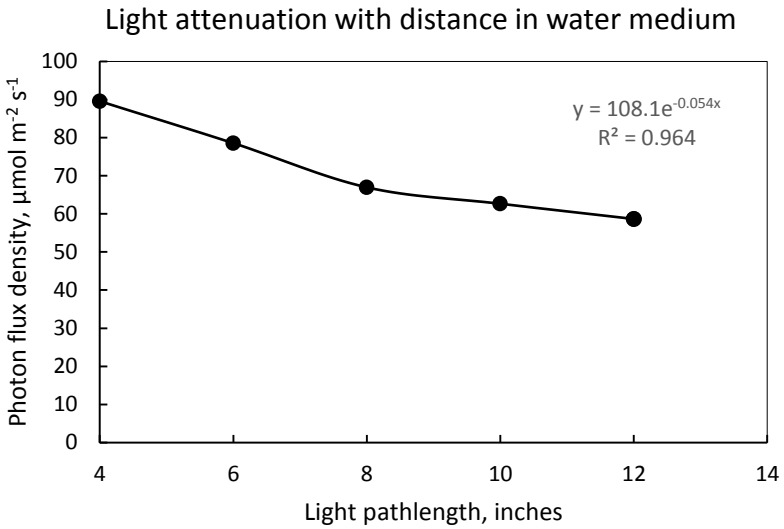

Figure 4.2. Light attenuation with path length

4.1.2. Phase 2: Interaction of light with gas bubbles

As shown in figure 4.1, the light attenuates with the increase in the bubble flume concentration in the PBR volume. Shanmoun et al (1999) suggested that the light attenuation with bubbles is the function of bubble concentration. The light attenuation is calculated by using output irradiance and input irradiance. In this case, input irradiance is considered as the output irradiance with no bubbles. For example, in the 102 mm PBR, 89.53 µmol m^{-2} s^{-1} is taken as input irradiance.

From figure 4.3, it can be seen that the patterns of light attenuation is almost the same among the photobioreactor light pathlengths. However, there are certain points that fall out of the pattern due to the scattering of light by the bubbles which cannot be uniform. With high air flow rate, the output light flux at the exit surface is low. Each individual bubble in the system acts as an optical lens which exhibits the optical

behaviors. As an optic material, the bubble tend to scatter the light that falls onto them in different directions.

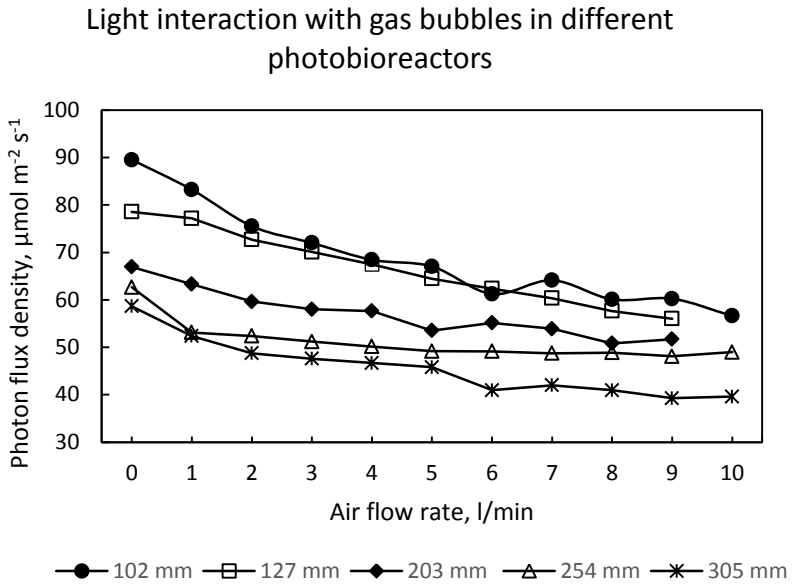

Figure 4.3. Light interactions with gas bubbles across different pathlengths

Table 4.3. Percentage of light attenuation with different rate of gas bubble flumes in different PBRs

Light attenuation percentage increase with different flow rates, (%)										
Flow rate, lpm										
Path length	1	2	3	4	5	6	7	8	9	10
102 mm	7.04	15.65	19.58	23.56	25.13	31.60	28.38	32.87	32.72	**36.76**
127 mm	1.76	7.49	10.80	14.09	17.94	20.61	23.20	26.63	28.69	**30.96**
203 mm	5.48	10.96	13.37	13.91	20.08	17.68	19.54	24.10	22.81	**24.83**
254 mm	15.21	16.38	18.28	19.98	21.49	21.55	22.23	22.00	23.23	**21.82**
305 mm	10.71	16.91	18.86	20.43	21.90	30.18	28.41	30.20	33.04	**32.52**

Table 4.3 shows the increase in light attenuation percentage with the introduction of gas bubbles with the different flow rates ranging from 1 l/min to 10 l/min.

In the 102 mm pathlength photobioreactor, the output light flux decreases from 89.53 to 56.62 μmol m^{-2} s^{-1} across the gas bubble flow rates from 0 l/min to 10 l/min that results in 37% light attenuation (table 4.3). In other words, the light flux decreases about 37% with 10 liters/min gas bubble flow when compared to no bubble flow. Similarly, in 305 mm photobioreactor, the output light flux decreases from 58.66 to 39.58 μmol m^{-2} s^{-1} that results in 33% light attenuation. The total light attenuation percentage across air flow rates (0 l/min to 10 l/min) in each photobioreactors (102 mm, 127 mm, 203 mm, 254 mm and 305 mm) ranges from 22% to 37%. The common phenomenon is that the light attenuates with the increase in air flow rates in all photobioreactor pathlengths. In figure 4.4, the drop in light intensity at 7 l/min of 102 mm PBR can be noticed as it is falling out of the pattern due to random scattering of light.

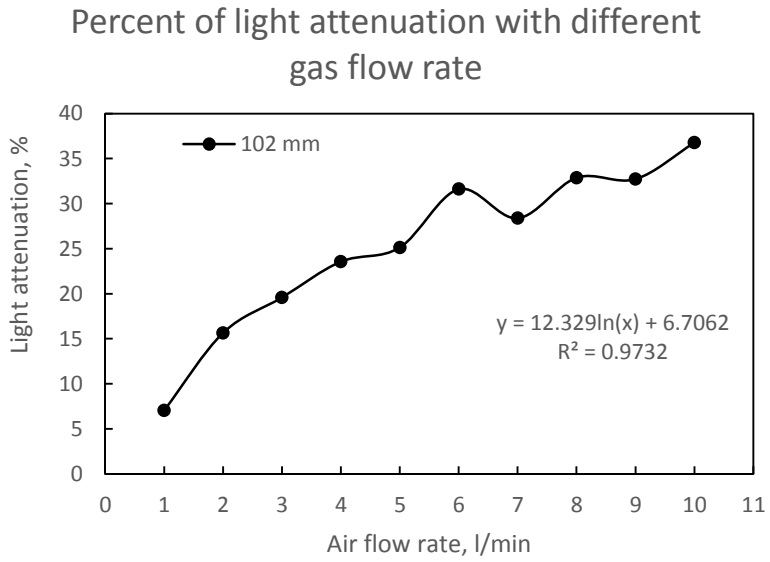

Figure 4.4. Light interaction with gas bubbles in the photobioreactor (102 mm)

The equation developed from the test data:

$$Output\ Irradiance,\ I_x = 84.16\ (\mu\text{mol m} - 2\ \text{s} - 1)\ e^{-0.042\ \left(bubble\ flow\ rate, \frac{l}{min}\right)} \quad (4.3)$$

4.1.3. Phase 3: Interaction of light with biomass concentration

Figure 4.5 shows the experiment setup of PBR system with the cultivation of microalgae. It can be seen that the light penetration in the high-density algal biomass medium. The incident light intensity of 229.54 μmol m^{-2} s^{-1} enters the front side of the PBR which travels the corresponding pathlength, for example, 102 mm pathlength.

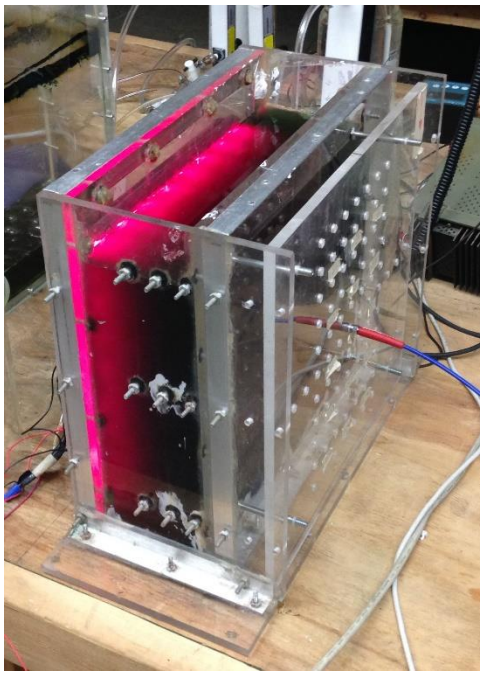

Figure 4.5. Light penetration into the high-density algal medium

The light attenuation calculation for the biomass is calculated by considering the output irradiance of water medium (198.21 μmol m^{-2} s^{-1}) as input irradiance for biomass.

This will help to eliminate the light attenuation with the distance in the calculations. The extinction coefficient of biomass is calculated using the equation 2.3.

Table 4.4. shows the light activity in the photobioreactor system with biomass.

Table 4.4. Light interaction with biomass in the medium of 102mm-photobioreactor

Biomass concentration, C_b ***kg/m^3***	**Initial light intensity, I_o** ***$\mu mol\ m^{-2}\ s^{-1}$***	**Final light intensity, I_x** ***$\mu mol\ m^{-2}\ s^{-1}$***	**Light attenuation, %**	**Extinction coefficient of biomass, a_c** ***m^2/g***
0.08	198.21	70.99	64.18	0.13
0.15	198.21	34.41	82.64	0.11
0.19	198.21	23.45	88.17	0.11
0.24	198.21	15.4	92.23	0.10
0.30	198.21	8.78	95.57	0.10
0.37	198.21	4.68	97.64	0.10
0.47	198.21	2.06	98.96	0.10
0.58	198.21	0.77	99.61	0.09
0.73	198.21	0.13	99.93	0.10
0.81	198.21	0.56	99.72	0.07
0.90	198.21	0.66	99.67	0.06
1	198.21	1.07	99.46	0.05

Figure 4.6 shows the light interaction with the suspended biomass in the photobioreactor system. In 102mm photobioreactor, light is passed through the medium which has suspended biomass and dissolved nutrients. In this case, light is absorbed by the biomass and the medium. As you can see in the figure 4.4, no light is passed through the system when the biomass concentration is 0.47 kg/m^3 and above.

The following equation developed from the test data:

$$I_x = 68.38(\mu\text{mol}\, m^{-2}\, s^{-1})\, e^{-5.961\ \left(biomass\ concentration, \frac{kg}{m^3}\right)} \quad (4.4)$$

Where, I_x = Output radiance, $\mu\text{mol}\, m^{-2}\, s^{-1}$

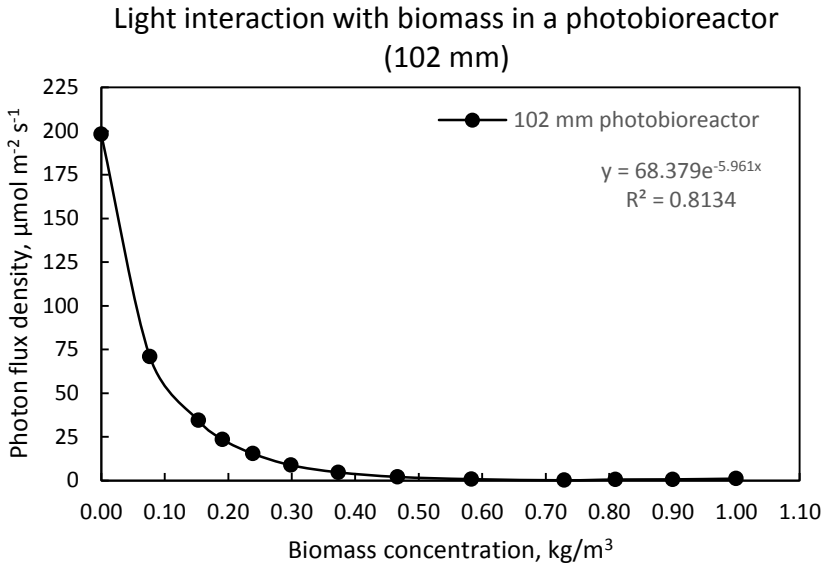

Figure 4.6. Light interaction with biomass in a photobioreactor (102 mm)

Based on the equation 2.3, the extinction coefficient of biomass is found out to be in the range of 0.05 to 0.13 $m^2\ g^{-1}$. Molina, et al. (2001) reported the extincition coefficient of biomass was 0.0396 $m^2\ g^{-1}$ for the biomass concentration of 1.9 kg m^{-3}. The result shows that the extinction coefficient found to be 0.05 $m^2\ g^{-1}$ for the biomass concentration of 1 kg m^{-3}.

4.2. Light guide test

The design factors of the light guides are diameter, length, taper angle and number of sections.

4.2.1. Effect of change in diameters of light guides

The diameter of a guide is directly related to its size (cross-sectional area). The change in diameter changes the size of the guide considerably. But as mentioned earlier, the change in diameter does not change the angles of reflection and refraction of light rays because of the shape of light guides. Diameters considered for the test are 9.53 mm, 25.4 mm and 50.8 mm (figure 4.7).

Light guides with a small diameter tend to have more ray interactions with the side surface. A light ray slightly loses energy at each interface interactions. With 9.53 mm light guides, the number of ray interactions with the side surface is more than that of light guides with 25.4 mm diameter and 50.8 mm diameter. Figure 4.7 shows that the number of interactions of a ray with the side surface increases with decrease in the diameter of a guide. It shows that if the ray enters in all three diameter guides with same incident angle, the interactions of ray along the side are one, two and six for the 50.8mm, 25.4 mm and 9.53 mm diameter light guides respectively. Moreover, the number of interactions can also be changed by the angle the refracted ray enters the input surface.

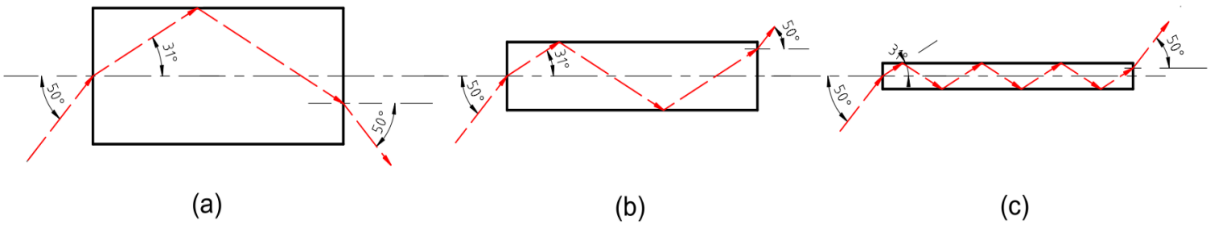

Figure 4.7. Propagation of a light ray in different sized light guides. a) 50.8 mm diameter, b) 25.4 mm diameter and c) 9.53 mm diameter light guide

For example, when a ray hits the light guide surface with an incident angle of 50°, it travels into a light guide 101.6 mm long with a refraction angle of 31° towards the

other end of the guide (figure 4.5). A light guide with 50.8 mm diameter has one interaction with the side surface whereas light guides with 25.4 mm and 9.53 mm have two and six interactions respectively. It implies that the light guides with a small diameter lose more energy than the light guides with a large diameter.

4.2.2. Effect of change in lengths of light guide

The length factor does not have influence on entrance angle of the rays transmission in the guide since the shape does not change. When the length of the guide increases, the number of interaction with side surfaces also increases. Lengths considered for the test are 100.6 mm, 152.4 mm and 203.2 mm. Since the variation of lengths between light guides are small, the number of ray interactions are also small for the various lengths. It leads to only a slight drop in the light energy when lengths of the guide is varied by 108 mm.

4.2.3. Effects of change in exit surface angles of light guides

The change in the exit surface angle changes the shape of the light guide unlike length and diameter. This results in varying the pattern of the light distribution at the light guide exit. The exit surface angles considered are 30°, 60° and 90°. The 90° angle makes the exit surface flat whereas 30° and 60° angles make the exit surface tapered. The change in the angle of the exit surface changes the incident angle of the rays at the exit surface, which can change the amount of light refracted out of the guide.

4.2.3.1. Light guide with 90° flat exit end

When a ray hits the 90° flat end output surface, most of it refracts out of the light guide at an angle (θ_4) which is equal to the angle of incident (θ_1) at the input surface

(figure 4.8). From table 4.2, it can be seen that the incident angle (θ_4) and refracted (θ_5) angles at the exit surface are 0° to 42.16° and 0° to 90° respectively. It can also be noted that the energy of output light is above 90% when the refracted light comes out at an angle less than 35°.

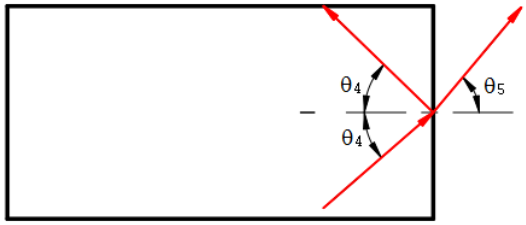

Figure 4.8.a. Ray exiting flat (90°) output surface.

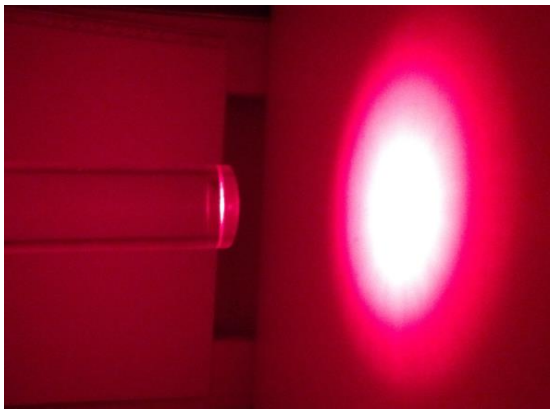

Figure 4.8.b. Distribution pattern of light guide from 90° flat end.

4.2.3.2. Light guide with 30° tapered exit end

When a ray hits the output surface, which has a taper angle of 30° to the light guide axis, part of it escapes from face-1, and the rest falls on face-2 (figure 4.9.a). All the reflected rays from face-1 hit face-2 where the most of the rays are refracted out of the guide. Figure 4.9.b shows the distribution pattern for light guide with 30° tapered surface. The cone-shaped output surface forms the wide distribution pattern. Table 4.7

shows the percent of light reflected back and refracted out of the light guides with a 30° tapered exit surface with incident, reflected and refracted angles.

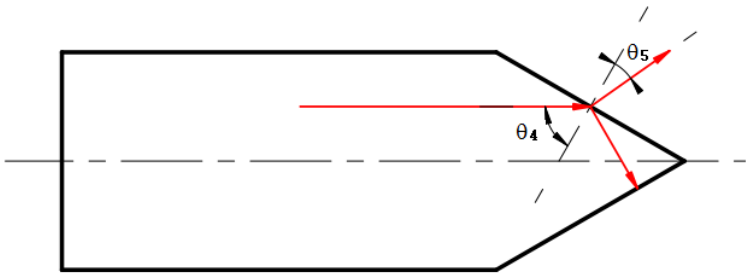

Figure 4.9.a. Ray exiting tapered (30°) output surface.

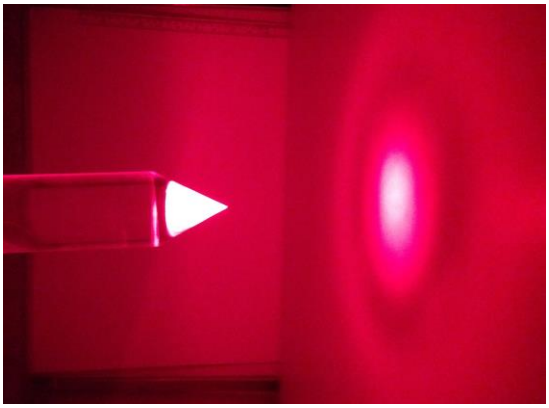

Figure 4.9.b. Distribution pattern of light guide from 30° tapered end.

4.2.3.3. Light guide with 60° tapered exit end

When a ray hits the output surface which has a taper angle of 60° to the light guide axis, most of the rays are refracted out and some rays are trapped inside the light guide.

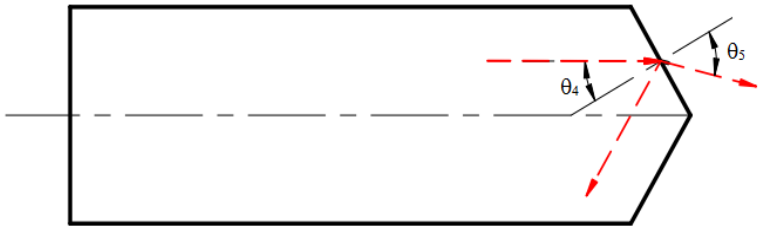

Figure 4.10.a. Ray exiting tapered (60°) output surface.

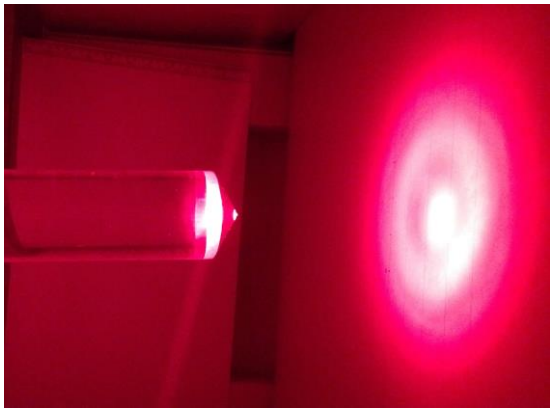

Figure 4.10.b. Distribution pattern of light guide from 60° tapered end.

4.2.4. Photon transmission efficiency of light guides

All 27 simple light guides are tested for photon transmission efficiency using the experimental optics system. Though simple light guides varied in shape and size, all are tested under common experimental conditions.

4.2.4.1.Case 1: Simple light guides

In the experiment, the amount of light supplied to a light guide is considered to be 100%. The amount of light exiting out of a light guide at the output surface and the side surface is measured with an integrating sphere and a spectrometer (table 4.5). The photon transmission efficiency of each light guide is then calculated as the percentage of amount of output light energy with respect to the input light energy which are measured in photonic units, µmol $m^{-2}s^{-1}$.

The results of these light guide tests are shown in the table 4.5. These results are compared and presented in graphical forms (figures 4.11 – 4.12). Since light guides have different geometrical shapes and sizes, each light guide shows different characteristics. However, light guides with common shapes and sizes show similar patterns. To

understand these characteristics of each light guides, the light guides are evaluated based on their photon transmission efficiency.

Table 4.5. Results of photon transmission efficiency of simple light guides.

Single-sectioned light guide								
Diameter		**Length**		**Exit taper angle**	**Light energy %**			
					Input energy	**Lost energy**	**Output energy**	
							Exit surface	**Side surface**
mm	*inches*	*Mm*	*inches*	*deg*				
(1)	*(2)*	*(3)*	*(4)*	*(5)*	*(6)*	*(7)*	*(8)*	*(9)*
50.8	2	101.6	4	30	100.00%	21.30%	76.41%	2.29%
				60	100.00%	27.74%	70.96%	1.30%
				90	100.00%	7.71%	90.17%	2.12%
50.8	2	152.4	6	30	100.00%	23.20%	75.75%	1.06%
				60	100.00%	31.06%	67.49%	1.44%
				90	100.00%	10.44%	89.45%	0.11%
50.8	2	203.2	8	30	100.00%	24.47%	74.27%	1.26%
				60	100.00%	30.64%	68.29%	1.06%
				90	100.00%	12.68%	86.30%	1.02%
25.4	1	101.6	4	30	100.00%	19.19%	78.43%	2.38%
				60	100.00%	25.93%	72.78%	1.29%
				90	100.00%	13.05%	86.17%	0.78%
25.4	1	152.4	6	30	100.00%	31.30%	67.81%	0.89%
				60	100.00%	33.18%	65.94%	0.89%
				90	100.00%	22.64%	77.02%	0.35%
25.4	1	203.2	8	30	100.00%	21.82%	77.37%	0.81%
				60	100.00%	28.64%	70.63%	0.73%
				90	100.00%	14.53%	85.36%	0.11%
9.53	⅜	101.6	4	30	100.00%	14.08%	70.46%	15.47%
				60	100.00%	13.31%	66.78%	19.91%
				90	100.00%	7.63%	75.07%	17.30%
9.53	⅜	152.4	6	30	100.00%	20.19%	63.98%	15.83%
				60	100.00%	17.24%	62.49%	20.27%
				90	100.00%	15.70%	65.97%	18.33%
9.53	⅜	203.2	8	30	100.00%	25.71%	55.60%	18.69%
				60	100.00%	35.52%	51.97%	12.51%
				90	100.00%	21.78%	64.10%	14.12%

Figure 4.11 shows the characteristics of light guides with diameter of 50.8 mm. Similarly, figures 4.11 to 4.13 show the characteristics of light guides with common diameters and common lengths.

The behavior of light guides with a common diameter and different lengths and different exit surface angles can be seen in the figures 4.11 – 4.13 that show the transmission efficiency of these light guides decreases with increases in lengths. For example, 50.8 mm diameter light guides have the transmission efficiency of 76.41%, 75.75% and 74.27% for 101.6 mm, 152.4 mm and 203.2 mm long light guides respectively. However, for the 25.4 mm diameter, it is not the case. It can also be noted that how shape of the exit surface influence the output. Generally, the transmission efficiency of light guides with a flat output end is high. Light guides with a tapered end are likely to have low transmission efficiency when compared to light guides with a flat end surface. Moreover, light guides with 30° tapered end have better transmission efficiency than light guides with 60° tapered end surface. For example, a light guide with 100.6 mm long and 50.5 mm diameter has a transmission efficiency of 90.17% with flat end, 76.41% with 30° tapered end and 70.96% with 60° tapered end.

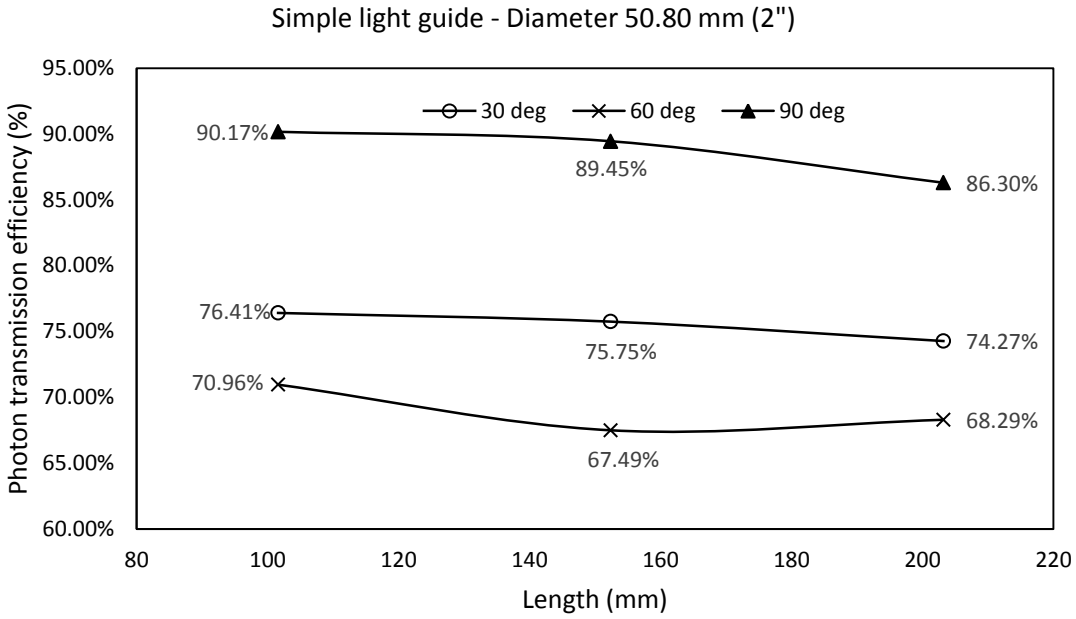

Figure 4.11. Photon transmission in 50.8 mm diameter simple light guides.

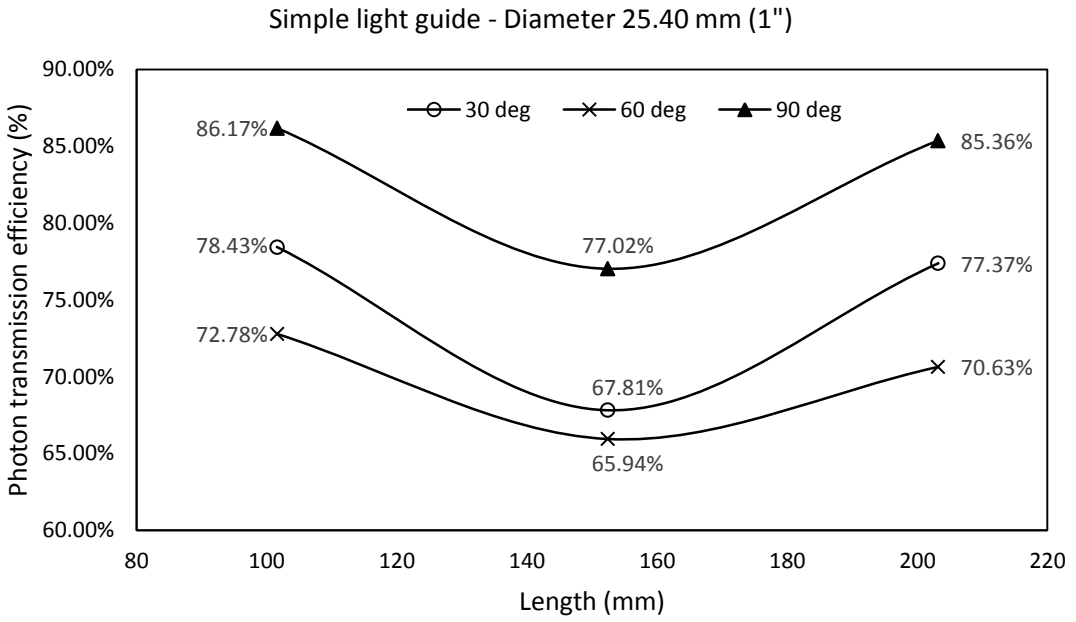

Figure 4.12. Photon transmission in 25.4 mm diameter simple light guides.

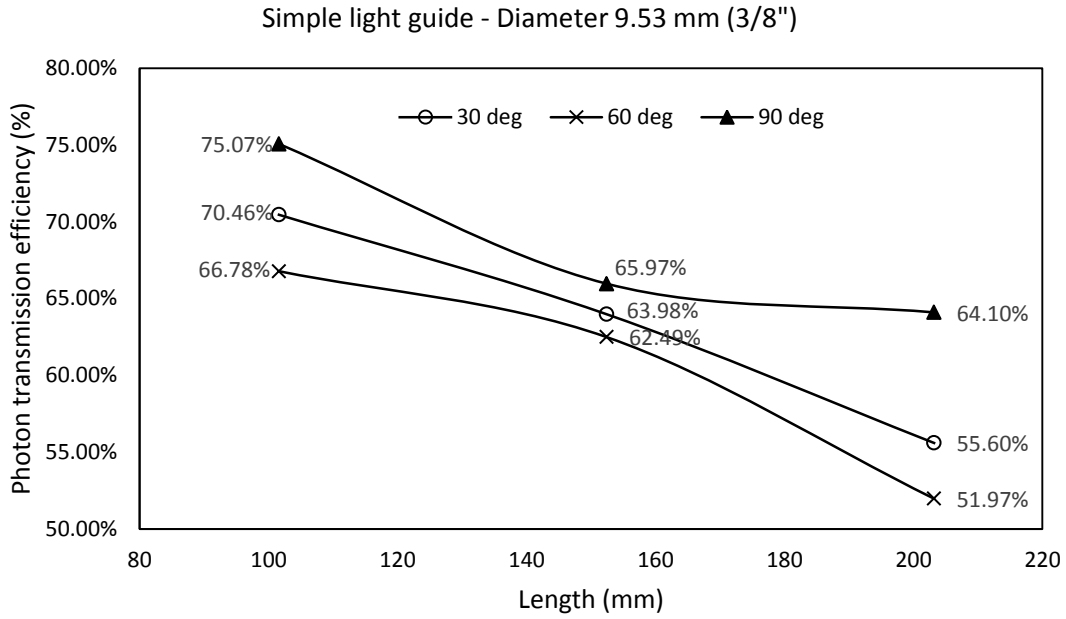

Figure 4.13. Photon transmission in 9.53 mm diameter simple light guides.

In contrary, there is a slight variation in the results of the 25.4 mm diameter light guides. Unlike the expected pattern, photon transmission efficiency of the 203.2 mm long light guide is lower than that of 152.4 mm long light guide as shown in the figure 4.13. According to the sizes, the transmission efficiency is directly related to the ratio of diameter and length of the light guide. These results commonly show that the transmission efficiency of a light guide is high when the ratio is high.

The following figures 4.14 to 4.16 show the effect on transmission efficiency of the changes in diameter of the light guides. Theoretically, transmission efficiency of a light guide increases with an increase in the diameter. The reduction in the size of a guide reduces the number of light ray interaction with the side surface internally which leads to loss of light energy. It is supported by the experimental results shown in figures 4.14 to 4.16, the light guide with 9.53 mm diameter has less photon transmission efficiency than the light guides with 25.4 mm diameter and 50.8 mm diameter. Comparatively, the light

guides with 50.8 mm diameter have more transmission efficiency than the light guides with 25.4 mm diameter. A similar result can also be seen in the 152.4 mm long light guides (figure 4.14). In contrast, the results of 100.6 mm long and 203.2 mm long light guides show a little variation in the trend unlike the former one. It can be seen in figures 4.14 and 4.16 that sometimes transmission efficiency of a light guide with 25.4 mm is slightly more than that of a light guide with 50.8 mm. However, the difference in the transmission efficiency of light guides with 25.4 mm diameter and 50.8 mm diameter is minimal because the variation in length of the guide is small in terms of the range of refraction angles of the light rays passing through the light guide and the number of ray interaction with the side surface internally.

Out of all 27 light guides, the maximum photon transmission efficiency of 90.17% is achieved with a 100.6 mm long flat-end light guide 50.8 mm in diameter.

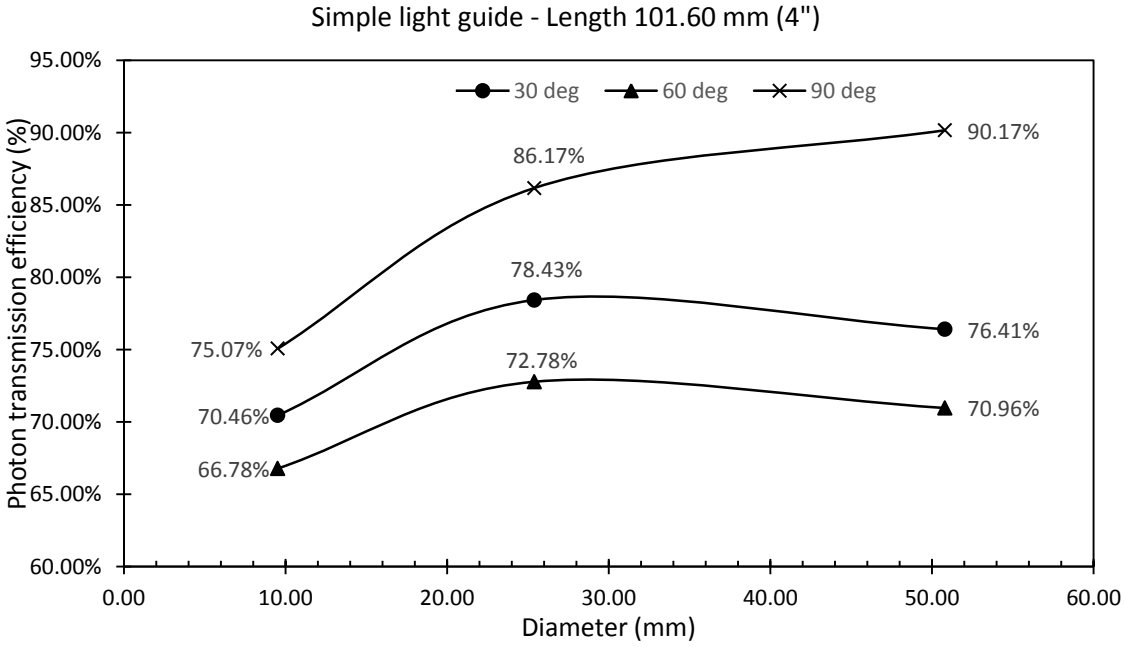

Figure 4.14. Photon transmission in 101.6 mm long simple light guides.

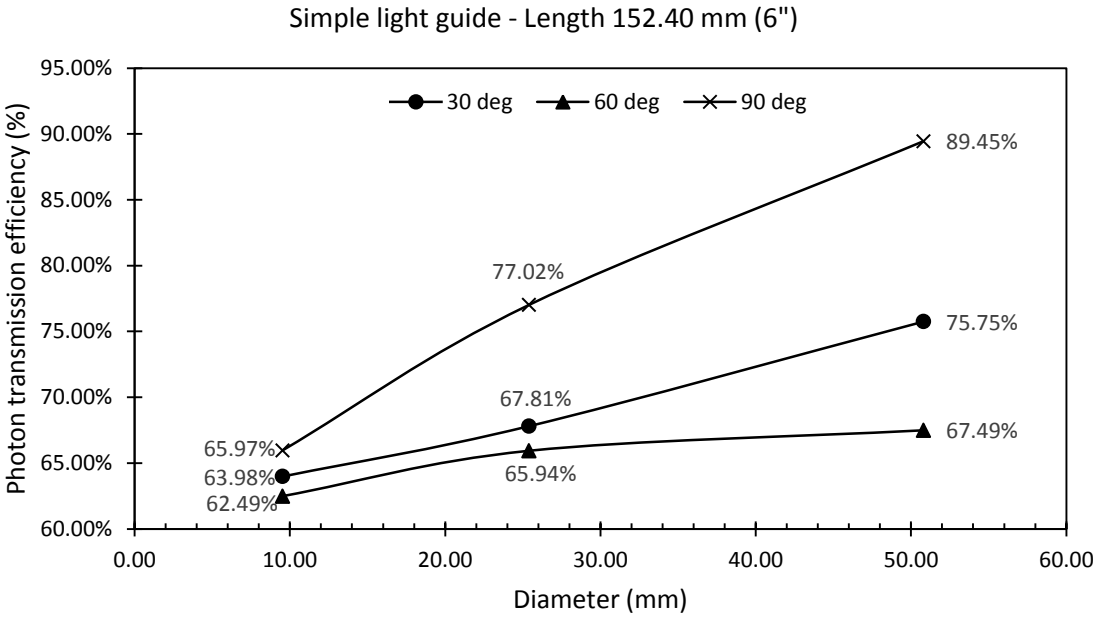

Figure 4.15. Photon transmission in 152.4 mm long simple light guides.

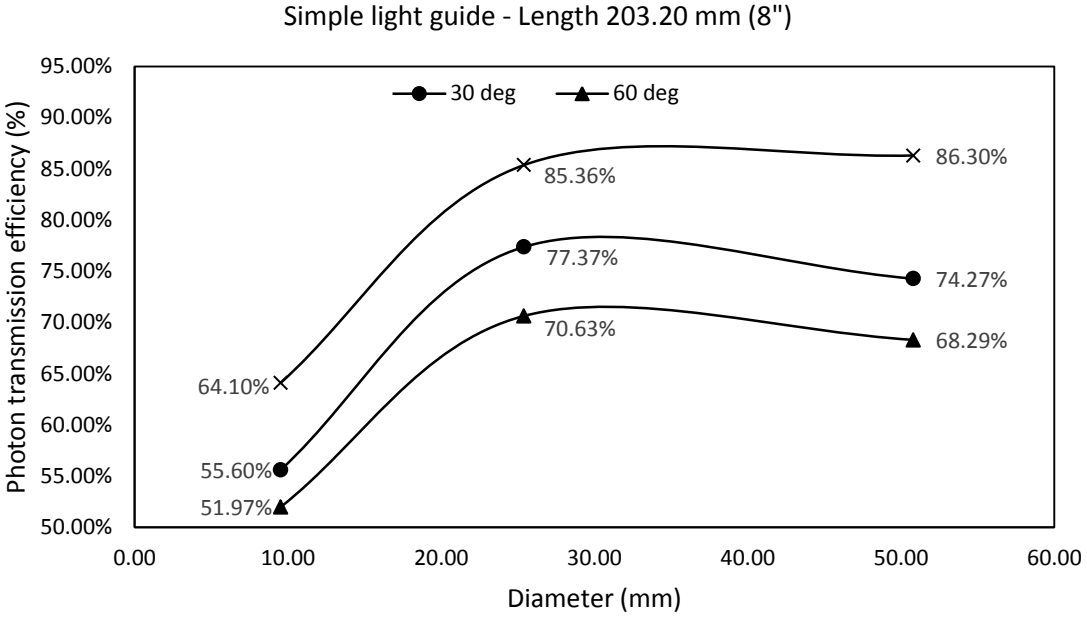

Figure 4.16. Photon transmission in 203.2 mm long simple light guides.

4.2.4.2. Case 2: Compound light guides

Compound light guides are categorized into two types, which are two-section light guides and three-section light guides. Two-section light guides have two output surfaces and three-section light guides have three output surfaces. Tests are conducted to measure the transmission efficiency of different light guides and the split of light energy between the two output surfaces.

4.2.4.3.Type 1: Two-sectioned light guide

The results of transmission efficiency of the two-section light guides is shown in the table 4.6 which shows the percent input energy of the light entering the guide and the percent of output energy escaping at each exit surface. Similar to simple light guides, the design factors of compound light guides are diameter, length and exit surface angle. Since it is a compound light guide, there are two sections with two exit surfaces and two different diameters. Under two-section light guides, two types of light guides can be made based on the sequence of sectional diameters. The sequences are 50.8 mm & 25.4 mm and 25.4 mm & 9.53 mm. With each sequence, nine light guides can be made with different lengths and different exit slope angles. These light guides can primarily be used to split the light energy through multiple exits.

Table 4.6. Results of photon transmission efficiency of two-section compound light guides.

Two-sectioned light guides								
Diameter combination	**Total length**	**Taper angle**	**Light energy (%)**					
			Input energy	**Lost energy**	**Output energy**			
					Section 1		***Section 2***	
mm	*mm*	*deg*			**Exit 1**	**Side 1**	**Exit 2**	**Side 2**
(1)	(2)	(3)	(4)	(5)	(6)	(7)	(8)	(9)
50.8 & 25.4	101.6	30	100.00%	13.47%	28.36%	0.54%	38.59%	19.04%
		60	100.00%	22.84%	42.10%	1.78%	29.48%	3.81%
		90	100.00%	9.27%	51.32%	0.64%	33.46%	5.31%
50.8 & 25.4	152.4	30	100.00%	21.91%	18.71%	2.02%	36.08%	21.28%
		60	100.00%	27.35%	34.60%	1.97%	28.09%	7.99%
		90	100.00%	17.00%	43.20%	1.37%	32.38%	6.04%
50.8 & 25.4	204.2	30	100.00%	21.44%	20.24%	2.91%	34.28%	21.12%
		60	100.00%	28.81%	35.74%	1.54%	26.76%	7.15%
		90	100.00%	14.76%	46.37%	0.98%	31.84%	6.06%
25.4 & 9.53	101.6	30	100.00%	14.65%	45.73%	5.13%	21.63%	12.86%
		60	100.00%	12.90%	49.46%	18.21%	14.62%	4.80%
		90	100.00%	7.70%	59.80%	12.36%	17.78%	2.36%
25.4 & 9.53	152.4	30	100.00%	15.62%	43.53%	10.17%	16.46%	14.22%
		60	100.00%	18.92%	54.77%	8.33%	13.00%	4.98%
		90	100.00%	11.51%	60.69%	8.82%	16.79%	2.18%
25.4 & 9.53	204.2	30	100.00%	20.42%	42.32%	7.46%	13.43%	16.37%
		60	100.00%	21.60%	45.82%	14.87%	12.71%	5.00%
		90	100.00%	17.59%	61.98%	2.25%	14.49%	3.69%

4.2.4.3.1. Sequence type-I: Light guides with sectional diameters (50.8 mm & 25.4 mm)

Figures 4.17 – 4.19 show the results of transmission efficiency of light guides with sectional diameters of 50.8 mm and 25.4 mm. Each figure shows the amount of light energy that escaped through both exits at different lengths. *Exit-1* is located in the section of large diameter (*section-I*) whereas *exit-2* located in the section of small diameter (*section-II*). Since both sections have equal lengths, the ratio between sectional diameter

and length are not equal. It implies that the section with high ratio has more transmission efficiency than the section with low ratio. Following figures (4.17 - 4.19) proves that most of the light energy escapes through *exit-1* when compared to *exit-2* irrespective of exit surface angles.

Figure 4.16 shows the results of transmission efficiency of the two-section light guides with flat exit surfaces. As in the simple light guide, the transmission efficiency of compound light guide decreases with increase in the length. Light energy splits at two exit surfaces of a light guide. By considering the input energy as 100%, the light energy at *exit-1* in *section-I* is 51.32% and at *exit-2* in *section-II* is to be 33.46% in a 100.6 mm long compound light guide. The rest of the energy is considered to be lost which is caused by back scattering (light leaving through entrance), Fresnel loss at input surface, and loss of light energy with distance.

It is noted that the *section-I* has a greater transmission efficiency than the *section-II.* Contrarily, the sequence type-I light guides with 30° tapered exit surfaces has a greater transmission efficiency in *section-II* than the *section-I* (figure 4.19).

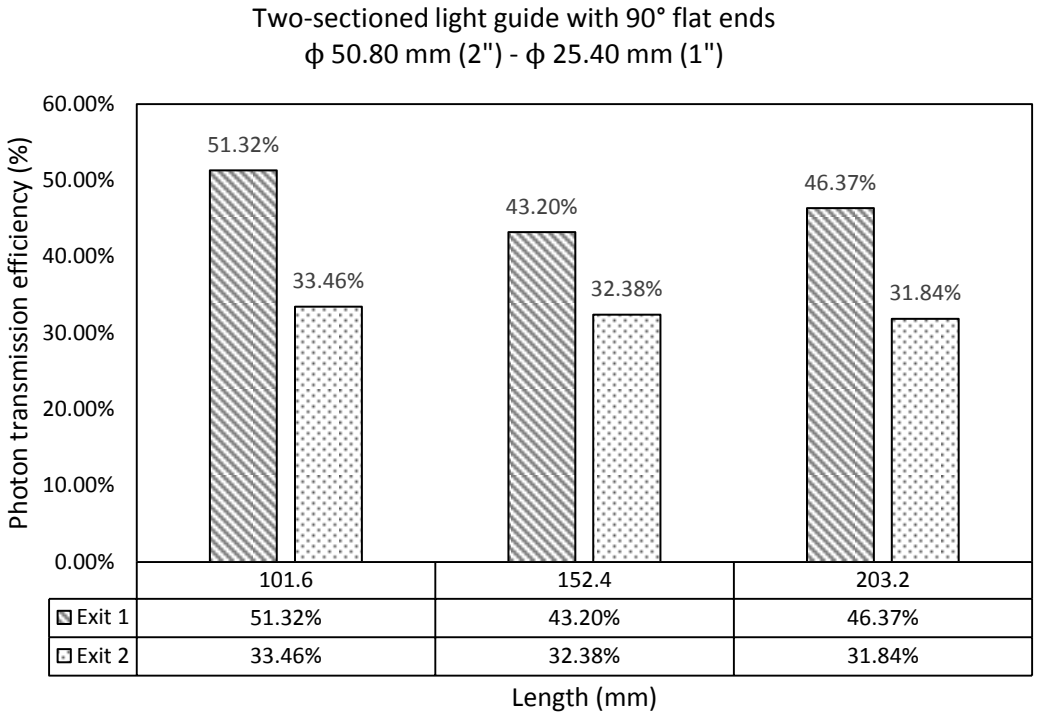

Figure 4.17. Photon transmission efficiency of sequence type-I two-sectioned light guides with two 90° flat exit surfaces.

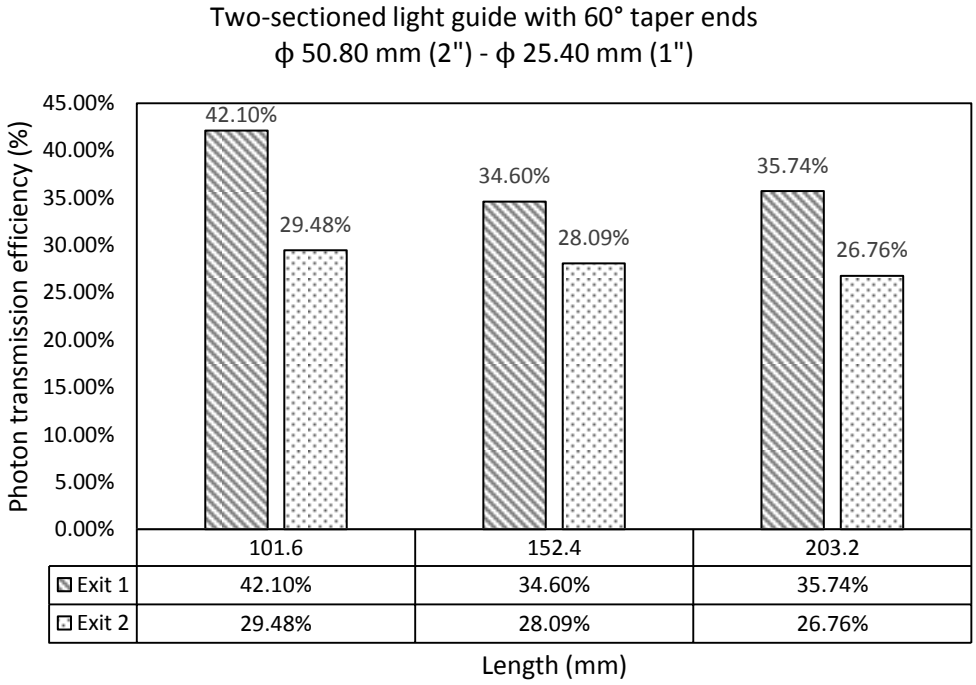

Figure 4.18. Photon transmission efficiency of sequence type-I two-sectioned light guides with two 60° taper exit surfaces.

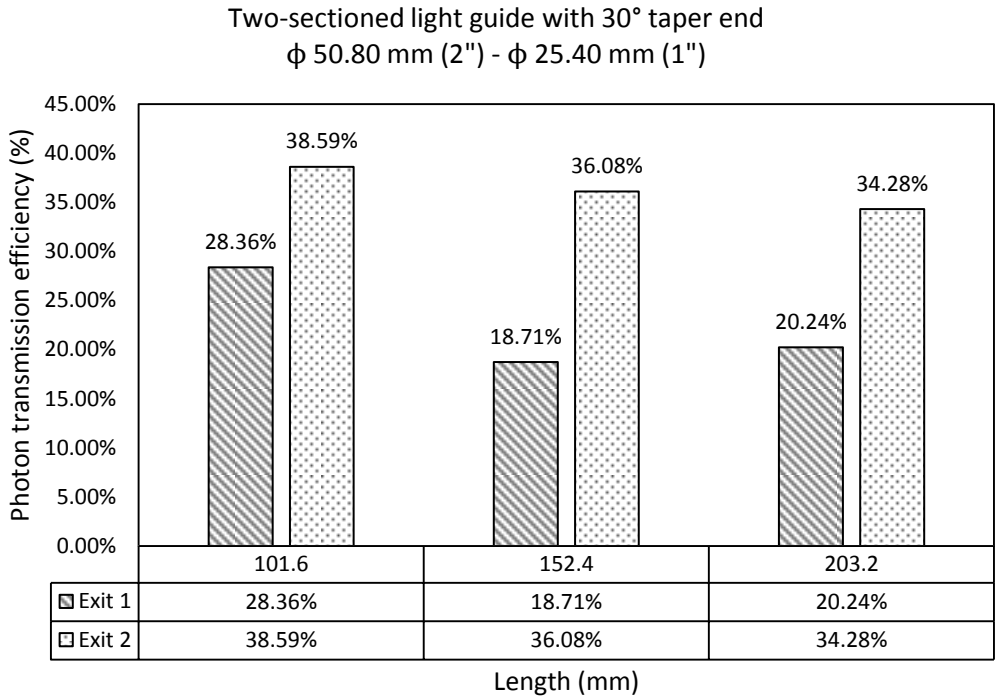

Figure 4.19. Photon transmission efficiency of sequence type-I two-sectioned light guides with two 30° taper exit surfaces.

4.2.4.3.2. Sequence type-2: Light guides with sectional diameters (25.4 mm & 9.53 mm)

Figures 4.20 – 4.22 show the transmission efficiency of sequence type-II light guides. Similar to sequence type-I, sequence type-II light guides have a similar pattern of splitting the light energy at two exit surfaces. Section-I has more transmission efficiency than section-II in all sequence type-II light guides.

Comparatively, the light energy output at *exit-1* of sequence type-I and sequence type-II light guides with flat exit surfaces at 101.6mm length is 51.32% and 59.80% respectively. The difference between light energy outputs at both exits is high in sequence type-II light guides. It is because of the high difference in the diameter-length ratio.

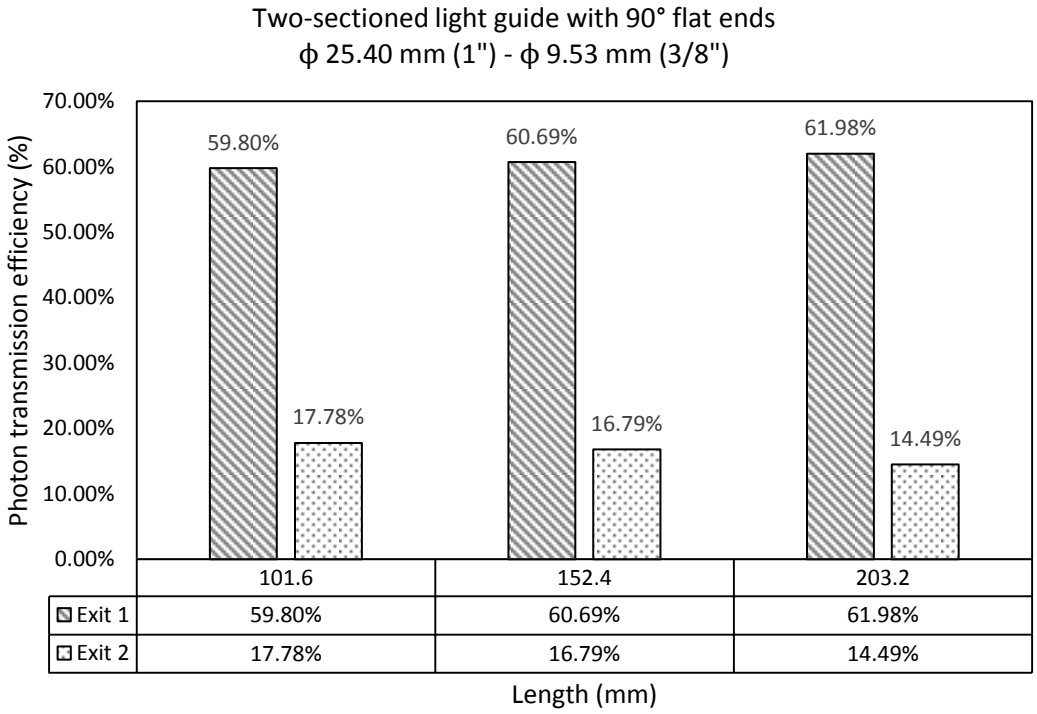

Figure 4.20. Photon transmission efficiency of sequence type-II two-sectioned light guides with two 90° flat exit surfaces.

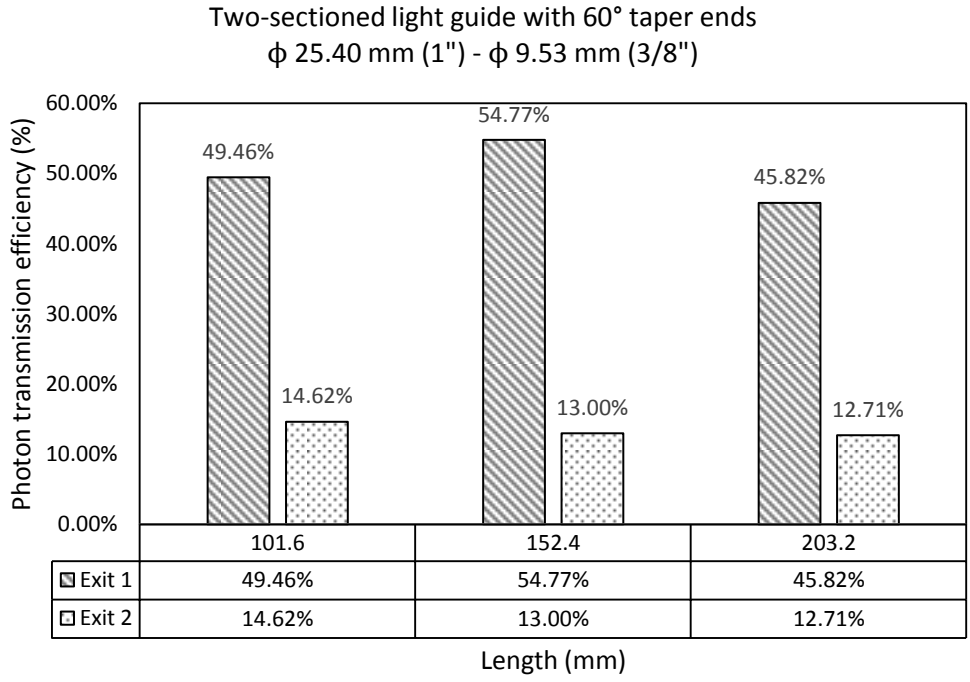

Figure 4.21. Photon transmission efficiency of sequence type-II two-sectioned light guides with two 60° taper exit surfaces.

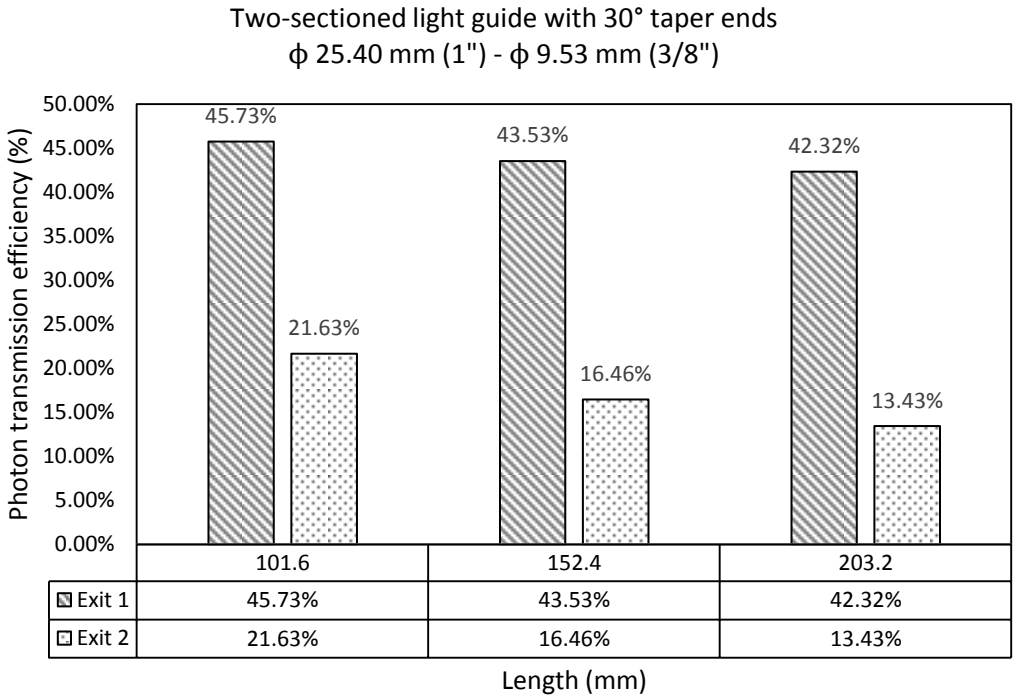

Figure 4.22. Photon transmission efficiency of sequence type-II two-sectioned light guides with two 30° taper exit surfaces.

4.2.4.4. Type 2: Three-section light guides

Table 4.7 shows the results of the photon transmission efficiency tests for the three-section light guides. As compound light guides, three-section light guides can split the light energy between three output locations/exit surfaces. These figures shows how light energy splits between three sections. The light energy always enters the light guide in the large section with diameter of 50.8 mm (section-1) and is transmitted along the sections with consequently smaller diameters 25.4 mm and 9.53 mm. As seen in figures 4.23 – 4.25, most of the light energy escapes through exit-1 since section-I has a high diameter and length ratio. Consequently, the remaining light energy escapes through exit-2 and exit -3. The light output at exit-3 is significantly low when comparted to the light output at exit-1 for all lengths of three-sectioned light guides.

As shown in following figures 4.23 – 4. 25, three-section light guides can output the light energy at about 40 – 50% at exit-1, 20 – 25 % at exit-2 and 5 – 10% at exit-3 respectively. Figure 4.23 shows the photon transmission efficiency of light guides with flat exit surfaces whereas figure 4.24 and 4.25 show the photon transmission efficiency of light guides with 30° and 60° taper exit surfaces. Three-sectioned light guides with 30° and 60° taper exit surfaces exhibit less transmission efficiency at exit-1 when compared to that of 90° flat exit surfaces. Especially, light guides with 30° taper exit surfaces have low transmission efficiency at all exits.

The amount of light energy exits out of exit-1 has slight variations with the increase in the length of the section. Additionally, the results show that the amount of lost light energy during transmission is high with the 60° tapered end light guide (table 4.7) which is common in simple and compound light guides.

Table 4.7. Results of photon transmission efficiency of three-sectioned compound light guides.

Three-sectioned light guides										
Diameter (mm)	**Length (mm)**	**Slope angle (deg)**	**Light energy (%)**							
			Input energy (%)	**Lost Energy (%)**	***Section 1***		***Section 2***		***Section 3***	
					Exit-1 (%)	**Side-1 (%)**	**Exit-2 (%)**	**Side-2 (%)**	**Exit-3 (%)**	**Side-3 (%)**
50.8 –	100.6	30	100.00	8.57	40.36	1.30	23.75	12.37	9.03	4.63
25.4 –		60	100.00	13.84	43.48	8.16	20.23	5.99	7.01	1.28
9.53		90	100.00	16.54	44.99	1.70	24.13	3.98	7.82	0.84
50.8 –	152.4	30	100.00	16.15	26.15	0.87	23.60	20.20	7.81	5.23
25.4 –		60	100.00	27.75	37.76	3.41	18.52	4.87	6.35	1.35
9.53		90	100.00	17.69	45.65	1.76	21.01	6.22	6.87	0.81
50.8 –	203.2	30	100.00	18.72	20.06	5.41	22.75	19.59	7.95	5.51
25.4 –		60	100.00	31.38	34.62	2.39	17.28	6.01	6.52	1.80
9.53		90	100.00	10.83	48.62	0.69	23.97	6.40	5.61	3.88

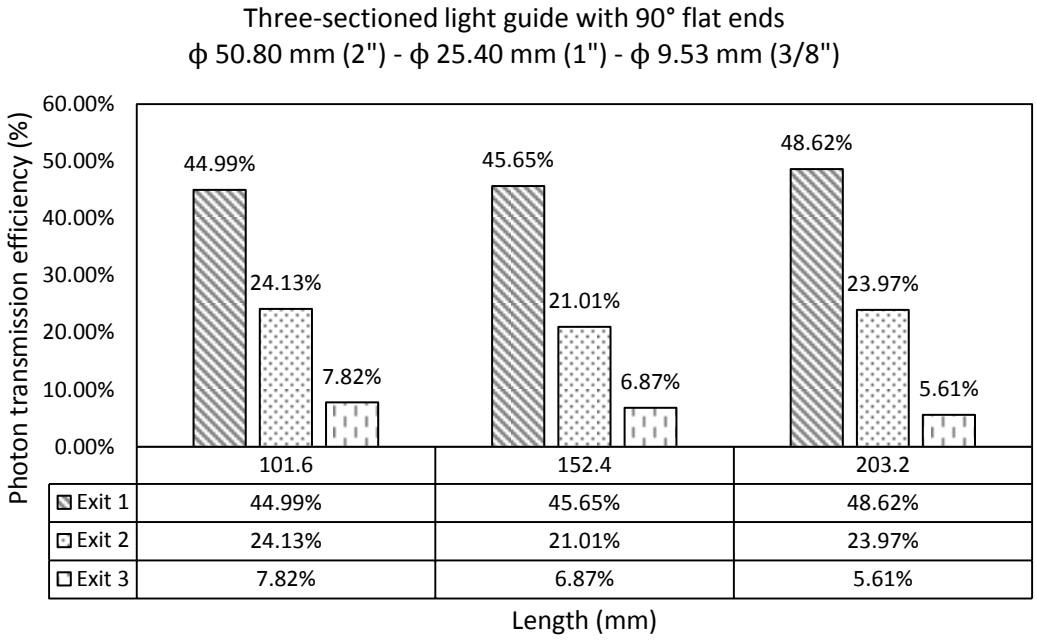

Figure 4.23. Photon transmission efficiency of three-sectioned light guides with three 90° flat exit surfaces.

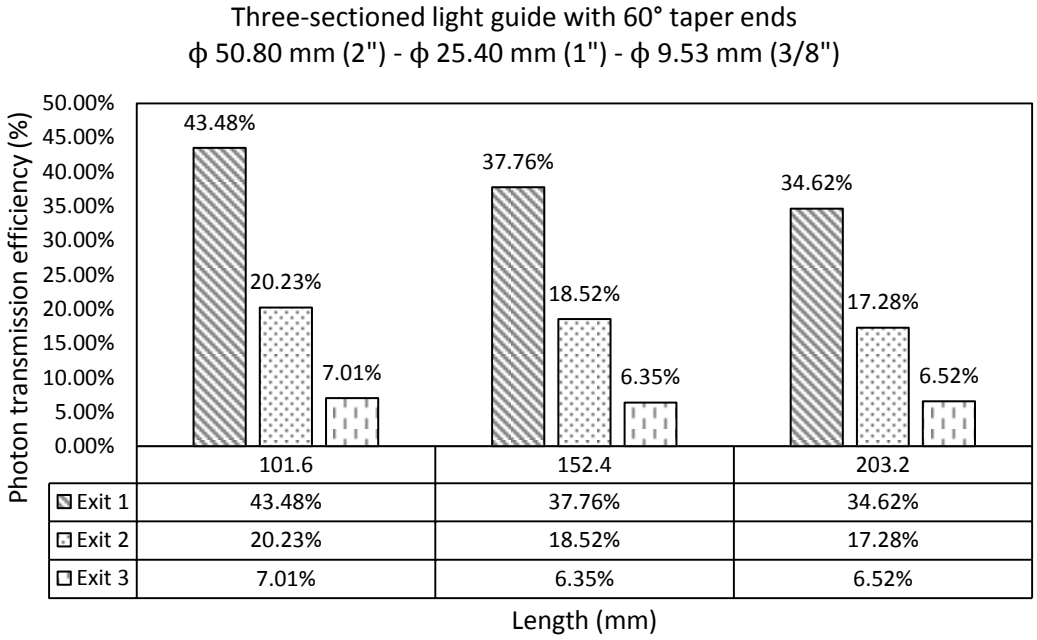

Figure 4.24. Photon transmission efficiency of three-sectioned light guides with three 60° taper exit surfaces.

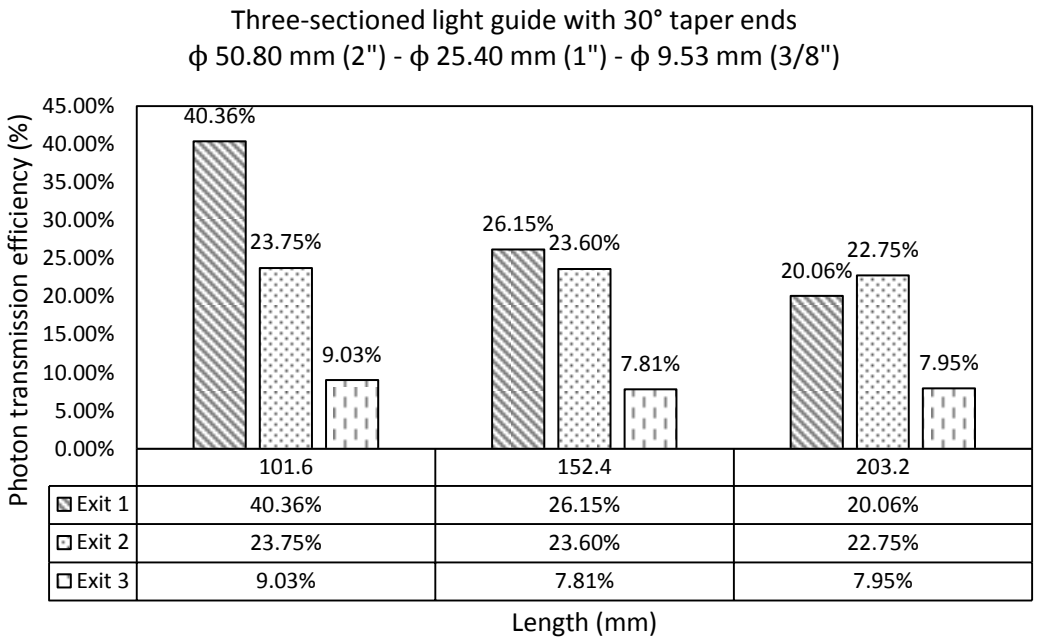

Figure 4.25. Photon transmission efficiency of three-sectioned light guides with three 30° taper exit surfaces.

Though most of the light guide characteristics are as predicted by theory expectations, there are few light guides which exhibit deviations in test results. Basically, there are lot of factors which affect the efficiency of light guides. Those factors could be the imperfection in the alignment of light guide in the experimental setup, slight imperfections in the shapes of light guide, the smoothness of the light guide surface, and the volume scattering.

5. CONCLUSIONS

The following conclusions can be drawn from the test results presented.

Interaction of light with the factors of PBR:

1. The light attenuation with path lengths relatively constant (30 – 37%) regardless of the sparger airflow rate which ranged from 0 – 10 lpm.
2. The sparger airflow rate and light path length effect on light attenuation is more linear than the attenuation due to algal biomass.
3. Light attenuates 15.80% in 102 mm path length PBR and 44.83% in 305 mm path length PBR. The extinction coefficient of water medium is found to be 0.002 m^{-1} which is comparatively low when compared to the value of Pope and Fry (1997), 0.0371 m^{-1}.
4. Light attenuates 7.04% with 1 lpm gas bubble flow rate in the water medium and 36.76% with 10 lpm gas bubble flow rate.
5. The impact of algal biomass on light attenuation is exponential.
6. Biomass settling may have changed the experimentally determined extinction coefficients for biomass in this study.
7. Extinction coefficients
    a. Light path length = 2 m^{-1}
    b. Gas bubbles = 0.41 min/m^4
    c. Biomass concentration = 51.2 – 131.7 m^2/kg
8. Equations
    a. Phase 1

$$Output\ Irradiance,\ I_x = 108.8\ (\mu mol\ m - 2\ s - 1)\ e^{-0.002\ x\ (depth,\ mm)}$$

b. Phase 2

$$I_x = 84.16\ (\mu\text{mol m} - 2\text{ s} - 1)\ e^{-0.042\ \left(bubble\ flow\ rate, \frac{l}{min}\right)}$$

c. Phase 3

$$I_x = 68.38(\mu\text{mol m} - 2\text{ s} - 1)\ e^{-5.961\ \left(biomass\ concentration, \frac{kg}{m^3}\right)}$$

Light guide test:

1. Light guide design factors are studied and analyzed theoretically.
    a. The transmission of light radiation is increased with increase in the diameter of the light guide.
    b. Transmission efficiency decreases with increase in the length of the light guide.
    c. Light is transmitted more in light guides with 90° flat exit surface than the light guides with 30° and 60° exit surface.
2. Photon transmission efficiency
    a. Transmission efficiency in simple light guides is found to be high in short light guides with large diameters.
    b. Observation of test results tells that about 50% of the light exits at the exit surface which is close to the incident illuminated surface.
    c. Simple light guide
        i. Highest transmission efficiency was found to be 90.17% in the light guide of 102mm long and 50.8 mm diameter with a 90^0 exit surface.

ii. Lowest transmission efficiency was found to be 51.97% in the light guide of 203 mm long and 9.53 mm diameter with a 60 ^{0} exit surface

d. Multi-section light guide

i. Highest transmission efficiency was found to be 84.88% in light guides with 102 mm long and 50.8 mm diameter with a 90^{0} exit surface. One cross section reduction.

ii. Lowest transmission efficiency was found to be 54.52% in light guides with 203.2 mm long and 50.8 mm diameter with a 30^{0} exit surface. One cross section reduction.

iii. Multi-section light guides emit more light at exit surface 1 than that at exit surface 2 and 3

iv. Multi-section light guides with a 30° exit taper surface are the exception

FUTURE WORK

1. Light guides will be tested in water medium as it is tested and analyzed in the air medium. The change in refractive index of the medium influences the behavior of the light guide.
2. The light guides will be incorporated in the flat-plate photobioreactor system and will be tested for illumination performance.
3. The flat-plate photobioreactor with light guides will be used to cultivate the microalgae. The specific growth rate of microalgae will be determined and compared with the specific growth rate of microalgae in flat-plate photobioreactor without light guides.

REFERENCES

Berg, J., Tymoczko, J., & Stryer , L. (2002). *Biochemistry.* New York: W H Freeman.

Brennan, L., & Owende, P. (2010). Biofuels from microalgae - A review of technologies for production, processing, and extractions of biofuels and co-products. *Renewable and Sustainable Energy Reviews, 14*, 557-577.

Bula, R., Morrow, R., Tibbitts, T., Barta , D., Ignatius, R., & Martin , T. (1991). Light-emitting diodes as a radiation source for plants. *HortScience, 26*(2), 203-205.

Carvalho, A. P., Silva, S. O., & Baptista, J. M. (2011). Light requirements in microalgal photobioreactors: an overview of biophotonic aspects. *Applied microbiology biotechnology*, 1275-1288.

Carvalho, A. P., Silva, S. O., Baptista, J. M., & Malcata, F. X. (2011). Light requirememts in microalgal photobioreactors: an overview of biophotonic aspects. *Applied microbiology biotechnology, 89*, 1275-1288.

Chisti, Y. (2007). Biodiesel from microalgae beats bioethanol. *Trends in Biotechnology, 26*(3), 126-131.

Chrismadha, T., & Borowitzka, M. A. (1994). Effect of cell density and irradiance on growth, proximate composition and eicosapentaenoic acid production of Phaeodactylum tricornutum grown in a tubular photobioreactor. *Journal of Applied Phycology, 6*, 67-74.

Clayton, R. K. (1970). *Light and Living Matter, Volume 1: The Physical Part.* New York: McGraw-Hill Book Company.

Dismukes, C. G., Carrieri, D., Bennette, N., Ananyev, G. M., & Posewitz, M. C. (2008). Aquatic phototrophs: efficient alternatives to land-based crops for biofuels. *Current Opinion in Biotechnology, 19*, 235-240.

Falkowski, P. G., & Raven, J. A. (1997). *Aquatic Photosynthesis.* Malden, Massachusetts, USA: Blackwell Science.

Grima, M., Fernandez, A., Camacho, G., & Chisti, Y. (1999). Photobioreactors: light regime, mass transfer, and scaleup. *Journal of Biotechnology, 70*, 231-247.

Grobbelaar, J. (2006). Photosynthetic response and acclimation of microalgae to light fluctuations In: Algal cultures anologues of blooms and applications. In D. Rao. Enfield (NH): Science Publishers.

Grobbelaar, J. U. (1994, June). Turbulence in mass algal culture and the role of light/dark fluctuations. *Journal of Applied Phycology, 6*(3), 331-335.

Grobbelaar, J. U. (2009). Factors governing algal growth in photobioreactors: the "open" versus "closed" debate. *Journal of applied phycology*, 489-492.

Gudin, C., & Chaumont, D. (1991). Cell fragility - The key problem of microalgae mass production in closed photobioreactors. *Bioresource Technology, 38*(2-3), 145-151.

Gupta, A., Lee, J., & Koshel, J. R. (2001). Design of efficient lightpipes for illumination by an analytical approach. *Applied optics, 40*(22), 3640-3648.

Iluz, D., & Dubinsky, Z. (2013). Quantum yields in Aquatic photosynthesis. In Z. Dubinsky, *Photosynthesis* (pp. 135-158). Croatia: Intech.

Janssen , M., Tramper , J., Mur, L., & Wijffels, R. (2003). Enclosed outdoor photobioreactors: light regime, photosynthetic efficiency, scale-up, and future prospects. *Biotechnol Bioeng*, 193-210.

Kirk, J. T. (1994). *Light and photosynthesis in aquatic ecosystems.* New york: Cambridge University Press.

Lee. (1999). Calculation of light penetration depth in photobioreactors. *Biotechnology bioprocessing engineering, 4*, 78-81.

Lee, C.-G., & Paisson, B. O. (1994). High-Density Algal Photobioreactors using Light-Emitting Diodes. *44*, 1161-1167.

Lee, C.-G., & Palsson, B. O. (1994). High-density algal photobioreactors using light-emitting diodes. *Biotechnology and bioengineering, 44*, 1161-1167.

Mohsenpour, S. F., Richards, B., & Willoughby, N. (2012). Spectral conversion of light for enhance microalgae growth rates and photosynthetic pigment production. *Bioresource Technology*, 75-81.

Molina, E., Fernandez, J., Acien, F., & Chisti, Y. (2001). Tubular photobioreactor design for algal cultures. *Journal of Biotechnology, 92*, 113-131.

Nielsen, E. (1966). The uptake of free CO2 and HCO3 - during photosynthesis of plankton alage with special reference to the coccolithophorid Coccolithus hurley. *Physiology Plant., 19*, 232-240.

Ogbonna, J. C., & Tanaka, H. (2000). Light requirement and photosynthetic cell cultivation - Developement of processes for efficient light utilization in photobioreactors. *Journal of Applied Phycology*, 207-218.

Ogbonna, J. C., & Tanaka, H. (2000). Light requirement and photosynthetic cell cultivation - Development of processes for efficient light utilization in photobioreactors. *Journal of Applied Phycology, 12*, 207-218.

Osborne, B. A., & Geider, R. J. (1987). The minimum photon requirement for photosynthesis. *New Phytology, 106*, 631-644.

Park, K.-H., & Lee, C.-G. (2001). Effectiveness of flashing light for increasing photosynthetic efficiency of microalgal cultures over a critical cell density. *Biotechnology Bioprocess Engineering, 6*, 189-195.

Pope, R. M., & Fry, E. S. (1997). Absorption spectrum (380 - 700 nm) of pure water. II. Integrating cavity measurement. *Applied optics, 36*(33), 8710-8723.

Pulz, O., & Scheibenbogen, K. (1998). Photobioreactors: Design and performance with respect to light energy input. *Advances in Biochemical Engineering/Biotechnology, 59*, 123-152.

Qiang, H., & Richmond, A. (1996). Productivity and photosynthetic efficiency of Sprirulina platensis as affected by light intensity, algal density and rate of mixing in a flat plat photobioreactor. *Journal of Applied Phycology, 8*, 139-145.

Qiang, H., Zarmi, Y., & Richmond, A. (1998). Combined effects of light intensity, light-path and culture density on output rate of Spirulina platensis (Cyanobacteria). *European Journal od Phycology, 33*(2), 165-171.

Rubio, F., Camacho, F., Sevilla, J., Chisti, Y., & Grima, E. (2003). A mechanistic model of photosynthesis in Microalgae. *Biotechnology and Bioengineering, 81*(4), 459-473.

Shamoun, B., Beshbeeshy, M., & Bonazza, R. (1999). Light extinction technique for void fraction measurements in bubbly flow. *Experiments in fluids*, 16 - 26.

Suh, I. S., & Lee, C.-G. (2003). Photobioreactor Engineering: Design and Performance. *Biotechnology and Bioprocess Engineering, 8*, 313-321.

Whithead, L., Nodwell, L., & Curzon, F. (1982). New efficient light guide for interior illumination. *Applied optics, 21*(15), 2755-2757.

Yasushi, K. (1991). New trends in photobiology: Structures and functions of carotenoids in photosynthetic systems. *Journal of photochemistry and photobiology B: Biology, 9*(3-4), 265-280.

Zijffers, J.-W. F., Janssen, M., Tramper, J., & Wijffels, R. H. (2008). Design process of an area-efficient photobioreactor. *Mar Biotechnol*, 404-415.

APPENDIX - A

Amount of light reflected and refracted with an incident angle and refracted angle of both interfaces in 90° flat end light guides

Air to acrylic glass interface				Acrylic glass to air interface			
Entry surface				Flat exit surface			
Incident angle	**Refracted angle**	**Reflected light**	**Refracted light**	**Incident angle**	**Refracted angle**	**Reflected light**	**Refracted light**
deg	*deg*	*%*	*%*	*Deg*	*deg*	*%*	*%*
0.00	0.00	0.00	100.00	0.00	0.00	0.00	100.00
5.00	3.35	3.87	96.13	3.35	5.00	3.87	96.13
10.00	6.69	3.87	96.13	6.69	10.00	3.87	96.13
15.00	10.00	3.88	96.12	10.00	15.00	3.88	96.12
20.00	13.27	3.90	96.10	13.27	20.00	3.90	96.10
25.00	16.48	3.94	96.06	16.48	25.00	3.94	96.06
30.00	19.61	4.02	95.98	19.61	30.00	4.02	95.98
35.00	22.64	4.17	95.83	22.64	35.00	4.17	95.83
40.00	25.56	4.44	95.56	25.56	40.00	4.44	95.56
45.00	28.33	4.88	95.12	28.33	45.00	4.88	95.12
50.00	30.94	5.62	94.38	30.94	50.00	5.62	94.38
55.00	33.35	6.82	93.18	33.35	55.00	6.82	93.18
60.00	35.54	8.75	91.25	35.54	60.00	8.75	91.25
65.00	37.46	11.87	88.13	37.46	65.00	11.87	88.13
70.00	39.10	16.92	83.08	39.10	70.00	16.92	83.08
75.00	40.41	25.12	74.88	40.41	75.00	25.12	74.88
80.00	41.37	38.60	61.40	41.37	80.00	38.60	61.40
85.00	41.96	61.17	38.83	41.96	85.00	61.17	38.83
90.00	42.16	100.00	0.00	42.16	90.00	100.00	0.00

APPENDIX - B

Amount of light reflected and refracted with an incident angle and refracted angle of both interfaces in 60° taper end light guides

Air to acrylic glass interface				Acrylic glass to air interface			
Entry Surface				60° Tapered exit surface			
Incident angle	**Refracted angle**	**Reflected light**	**Refracted light**	**Incident angle**	**Refracted angle**	**Reflected light**	**Refracted light**
deg	*deg*	*%*	*%*	*Deg*	*deg*	*%*	*%*
0	0.00	0.00	100.00	30.00	48.16	5.31	94.69
5	3.35	3.87	96.13	26.65	41.93	4.58	95.42
10	6.69	3.87	96.13	23.31	36.12	4.22	95.78
15	10.00	3.88	96.12	20.00	30.63	4.04	95.96
20	13.27	3.90	96.10	16.73	25.40	3.94	96.06
25	16.48	3.94	96.06	13.52	20.39	3.90	96.10
30	19.61	4.02	95.98	10.39	15.59	3.88	96.12
35	22.64	4.17	95.83	7.36	11.00	3.87	96.13
40	25.56	4.44	95.56	4.44	6.63	3.87	96.13
45	28.33	4.88	95.12	1.67	2.49	3.87	96.13
50	30.94	5.62	94.38	-0.94	-1.40	3.87	96.13
55	33.35	6.82	93.18	-3.35	-5.00	3.87	96.13
60	35.54	8.75	91.25	-5.54	-8.27	3.87	96.13
65	37.46	11.87	88.13	-7.46	-11.16	3.87	96.13
70	39.10	16.92	83.08	-9.10	-13.63	3.88	96.12
75	40.41	25.12	74.88	-10.41	-15.62	3.88	96.12
80	41.37	38.60	61.40	-11.37	-17.09	3.89	96.11
85	41.96	61.17	38.83	-11.96	-17.98	3.89	96.11
90	42.16	100.00	0.00	-12.16	-18.28	3.89	96.11

APPENDIX - C

Amount of light reflected and refracted with an incident angle and refracted angle of both interfaces in 30° taper end light guides

Air to acrylic glass interface				Acrylic glass to air interface							
Entry surface				Exit surface (30° taper angle) - 1st face				Exit surface (30° taper angle) - 2nd face			
Incident angle	**Refracted angle**	**Reflected light**	**Refracted light**	**Incident angle**	**Refracted angle**	**Reflected light**	**Refracted light**	**Incident angle**	**Refracted angle**	**Reflected light**	**Refracted light**
deg	*deg*	*%*	*%*	*deg*	*deg*	*%*	*%*	*deg*	*deg*	*%*	*%*
0	0.00	0.00	100.00	60.00	0.00	100.00	0.00	0.00	0.00	0.00	100.00
5	3.35	3.87	96.13	56.65	0.00	100.00	0.00	3.35	5.00	3.87	96.13
10	6.69	3.87	96.13	53.31	0.00	100.00	0.00	6.69	10.00	3.87	96.13
15	10.00	3.88	96.12	50.00	0.00	100.00	0.00	10.00	15.00	3.88	96.12
20	13.27	3.90	96.10	46.73	0.00	100.00	0.00	13.27	20.00	3.90	96.10
25	16.48	3.94	96.06	43.52	0.00	100.00	0.00	16.48	25.00	3.94	96.06
30	19.61	4.02	95.98	40.39	74.92	24.95	75.05	19.61	30.00	4.02	95.98
35	22.64	4.17	95.83	37.36	64.71	11.65	88.35	22.64	35.00	4.17	95.83
40	25.56	4.44	95.56	34.44	57.43	7.64	92.36	25.56	40.00	4.44	95.56
45	28.33	4.88	95.12	31.67	51.47	5.91	94.09	28.33	45.00	4.88	95.12
50	30.94	5.62	94.38	29.06	46.37	5.05	94.95	30.94	50.00	5.62	94.38
55	33.35	6.82	93.18	26.65	41.94	4.58	95.42	33.35	55.00	6.82	93.18
60	35.54	8.75	91.25	24.46	38.10	4.32	95.68	35.54	60.00	8.75	91.25
65	37.46	11.87	88.13	22.54	34.82	4.17	95.83	37.46	65.00	11.87	88.13
70	39.10	16.92	83.08	20.90	32.11	4.08	95.92	39.10	70.00	16.92	83.08
75	40.41	25.12	74.88	19.59	29.97	4.02	95.98	40.41	75.00	25.12	74.88
80	41.37	38.60	61.40	18.63	28.42	3.99	96.01	41.37	80.00	38.60	61.40
85	41.96	61.17	38.83	18.04	27.48	3.97	96.03	41.96	85.00	61.17	38.83
90	42.16	100.00	0.00	17.84	27.17	3.97	96.03	42.16	90.00	100.00	0.00

APPENDIX - D

Output light flux measured at 15 positions in the grid during the experiment phase 1 and 2

Light Intensity Measurements (µmol m^{-2} s^{-1})																	
Air flow rate, lpm	**Rows**		**4"**			**6"**			**8"**			**10"**			**12"**		
			Columns			Columns			Columns			Columns			Columns		
			C 1	C 2	C 3	C 1	C 2	C 3	C 1	C 2	C 3	C 1	C 2	C 3	C 1	C 2	C 3
		Position	**-2**	**0**	**2**	**-2**	**0**	**2**	**-2**	**0**	**2**	**-2**	**0**	**2**	**-2**	**0**	**2**
0	R 1	**4**	52.08	52.97	49.63	62.63	67.33	64.03	54.18	57.28	59.33	46.51	47.56	45.52	44.62	45.58	44.85
	R 2	**2**	74.73	75.14	70.78	71.64	78.13	74.81	63.00	67.81	68.40	55.26	57.22	54.96	54.13	56.66	54.46
	R 3	**0**	86.30	89.53	84.69	71.16	78.56	75.71	62.94	66.97	66.82	60.30	62.66	60.35	56.03	58.66	57.25
	R 4	**-2**	81.23	82.51	78.88	69.37	74.94	73.13	59.21	64.50	64.32	59.82	61.48	59.14	54.64	56.85	55.06
	R 5	**-4**	67.54	70.13	68.38	64.24	70.03	66.05	53.80	57.97	56.81	57.79	60.28	56.74	44.62	53.32	52.06
1	R 1	**4**	48.81	49.32	47.37	50.89	54.87	50.51	40.85	44.32	47.11	37.58	39.52	39.58	39.77	41.61	40.79
	R 2	**2**	70.68	70.75	68.06	69.45	75.77	70.29	56.97	63.23	63.64	45.17	47.18	46.87	46.44	48.85	47.95
	R 3	**0**	80.75	83.23	81.19	69.76	77.18	72.66	58.65	63.30	64.13	49.85	53.13	51.79	49.33	52.38	52.75
	R 4	**-2**	75.72	77.17	76.70	67.97	73.58	70.17	55.52	60.65	62.03	52.38	55.00	54.73	49.50	51.69	51.17
	R 5	**-4**	62.71	65.92	66.79	50.89	68.69	62.99	49.51	54.24	54.57	51.36	54.38	53.36	46.73	48.84	48.90
2	R 1	**4**	44.56	45.81	44.51	44.68	48.53	44.82	48.19	53.72	54.49	34.03	37.16	37.04	35.46	37.57	38.12
	R 2	**2**	63.64	66.48	64.50	63.40	69.83	65.45	55.64	60.37	60.98	43.23	45.41	45.37	42.74	45.08	44.73
	R 3	**0**	73.65	75.52	76.08	64.85	72.67	68.27	54.88	59.63	61.05	48.90	52.40	52.43	46.59	48.74	50.21
	R 4	**-2**	70.93	60.80	64.51	63.36	64.49	58.44	52.81	51.95	52.33	51.07	52.92	52.75	46.48	46.63	47.82
	R 5	**-4**	58.34	73.20	74.48	57.80	69.29	65.70	46.67	58.57	59.60	49.43	54.14	54.63	44.78	49.05	49.85
3	R 1	**4**	43.17	43.34	42.63	41.27	45.69	55.38	34.90	38.01	52.29	34.90	38.01	52.29	33.60	34.82	35.52
	R 2	**2**	62.18	63.66	62.57	60.07	66.66	61.43	51.45	55.78	57.89	51.45	55.78	57.89	41.63	43.09	42.71
	R 3	**0**	70.78	72.00	73.61	63.07	70.07	65.35	53.23	58.01	59.75	53.23	58.01	59.75	45.32	47.60	48.91
	R 4	**-2**	67.68	57.82	60.21	60.97	61.47	56.18	50.35	49.85	49.79	49.74	51.94	52.64	46.06	46.25	46.97
	R 5	**-4**	54.88	70.33	71.49	55.16	67.09	63.35	44.80	55.91	57.50	48.85	53.53	54.48	44.79	47.79	48.65

4	R 1	**4**	41.83	41.45	40.63	39.88	42.87	39.86	33.97	37.16	39.15	33.97	37.16	39.15	32.42	33.86	33.93
	R 2	**2**	60.72	60.17	59.53	58.27	64.20	59.68	49.50	54.97	56.16	49.50	54.97	56.16	39.37	41.79	41.78
	R 3	**0**	66.90	68.44	69.70	61.00	67.49	62.95	52.67	57.65	58.23	52.67	57.65	58.23	43.57	46.68	47.85
	R 4	**-2**	64.69	54.58	58.92	59.15	59.72	53.82	49.12	49.25	49.10	49.12	49.25	49.10	45.08	46.26	46.84
	R 5	**-4**	52.42	66.72	67.52	53.52	65.30	60.70	44.27	55.22	56.12	44.27	55.22	56.12	44.75	47.00	48.42
5	R 1	**4**	38.85	38.99	37.51	37.29	53.42	37.43	33.14	32.96	37.38	30.53	32.35	32.34	30.54	32.14	33.31
	R 2	**2**	57.15	55.43	52.12	54.18	60.42	57.17	48.46	52.06	53.50	39.04	41.84	42.25	38.28	41.31	40.16
	R 3	**0**	63.58	67.03	62.34	58.51	64.46	60.68	51.50	53.52	57.14	44.49	49.19	49.83	42.22	45.81	46.17
	R 4	**-2**	58.36	51.67	53.44	56.20	57.20	51.55	48.52	47.59	47.51	46.88	48.12	48.85	42.96	45.30	46.53
	R 5	**-4**	48.03	62.45	62.43	50.76	62.46	58.34	43.42	53.58	55.42	44.30	51.93	52.75	41.96	46.26	47.66
6	R 1	**4**	37.82	39.16	37.70	35.20	38.33	36.49	32.01	33.19	35.56	29.96	32.12	31.00	26.62	29.13	29.44
	R 2	**2**	53.53	54.30	52.13	52.46	59.24	53.94	48.11	49.38	51.50	39.05	42.27	41.89	34.89	37.16	37.98
	R 3	**0**	61.44	61.24	60.05	55.93	62.37	57.66	51.66	55.13	54.64	44.91	49.16	50.59	39.97	40.95	43.00
	R 4	**-2**	56.91	48.31	51.14	54.43	55.20	49.80	47.39	47.67	46.94	47.14	48.07	47.78	41.07	40.91	42.71
	R 5	**-4**	43.96	60.76	59.16	48.82	60.77	56.67	42.05	53.51	53.57	43.58	51.24	52.33	38.87	43.58	44.09
7	R 1	**4**	39.20	39.27	39.21	44.02	36.84	34.80	30.78	33.58	34.84	29.73	33.18	32.51	26.26	28.07	28.59
	R 2	**2**	55.12	55.41	51.37	49.39	55.65	49.91	47.40	49.69	48.34	38.09	42.24	41.44	33.85	36.21	36.72
	R 3	**0**	61.89	64.13	63.82	52.67	60.33	56.81	50.46	53.88	54.91	43.30	48.73	48.82	38.20	42.00	42.04
	R 4	**-2**	56.54	49.97	53.36	52.53	53.61	48.27	46.35	45.38	46.67	45.99	47.23	47.05	38.77	40.15	41.10
	R 5	**-4**	45.57	61.05	62.14	46.78	57.62	55.01	41.60	52.45	53.48	42.14	50.27	50.27	38.00	41.53	43.56
8	R 1	**4**	36.79	36.15	36.55	31.44	34.33	32.65	30.64	33.50	34.77	31.31	32.77	33.84	26.40	27.66	28.12
	R 2	**2**	52.81	51.85	50.62	46.66	53.64	48.93	45.26	50.76	48.71	39.55	43.04	43.18	33.90	34.53	36.88
	R 3	**0**	60.20	60.10	60.24	51.40	57.64	55.48	50.01	50.83	52.26	44.67	48.87	48.75	38.20	40.95	41.22
	R 4	**-2**	56.18	47.69	50.07	51.00	51.11	46.88	46.88	45.28	45.59	46.80	46.52	47.94	39.79	40.12	41.61
	R 5	**-4**	43.76	56.35	59.98	44.54	56.17	54.05	41.50	49.47	52.29	43.92	51.59	51.41	37.64	41.21	43.77

9	R 1	**4**	37.40	36.98	36.05	28.92	32.64	31.22	31.19	33.36	34.34	29.83	32.56	32.17	25.62	27.33	26.37
	R 2	**2**	50.65	52.38	49.71	44.87	50.81	47.77	45.20	50.50	51.44	40.17	42.84	40.96	32.57	34.35	34.69
	R 3	**0**	55.39	60.23	56.67	49.52	56.02	52.88	49.53	51.69	54.06	43.66	48.11	50.01	37.24	39.28	40.73
	R 4	**-2**	51.71	56.27	56.67	50.11	55.48	52.57	46.76	51.38	52.39	45.01	48.80	49.12	37.38	41.07	42.14
	R 5	**-4**	37.40	45.54	48.56	43.34	49.73	44.16	41.47	45.40	44.54	40.94	45.18	46.03	36.86	39.43	40.72
10	R 1	**4**	35.39	37.32	36.51							29.75	30.86	30.86	25.40	26.29	26.99
	R 2	**2**	51.48	51.66	50.21							38.46	41.85	42.22	32.52	33.69	34.76
	R 3	**0**	54.59	56.62	59.98							44.90	48.99	50.61	37.06	39.58	39.65
	R 4	**-2**	42.40	46.14	48.25							40.08	43.59	45.01	35.81	39.02	39.78
	R 5	**-4**	52.08	56.30	57.04							44.50	49.08	49.03	37.46	40.35	42.20

APPENDIX - E

Depth of light penetration in the PBR system (102 mm pathlength) with different biomass concentration (descending order).

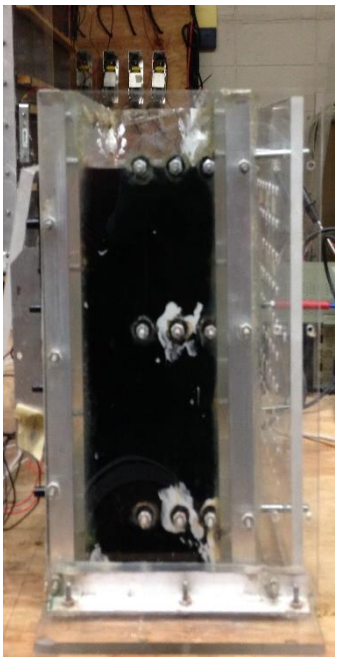

PBR system with biomass

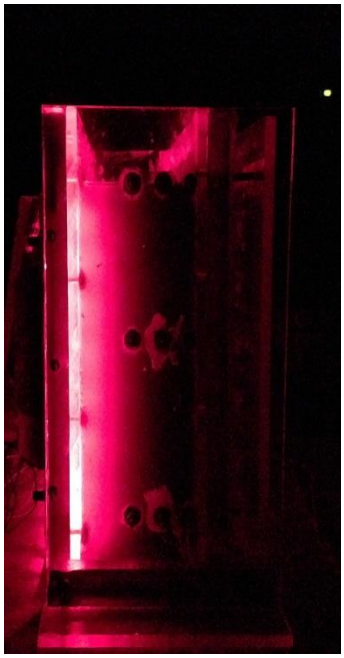

1 kg m^{-3}

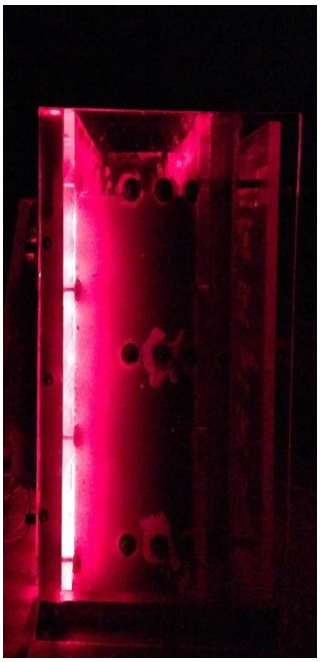

0.9 kg m^{-3}

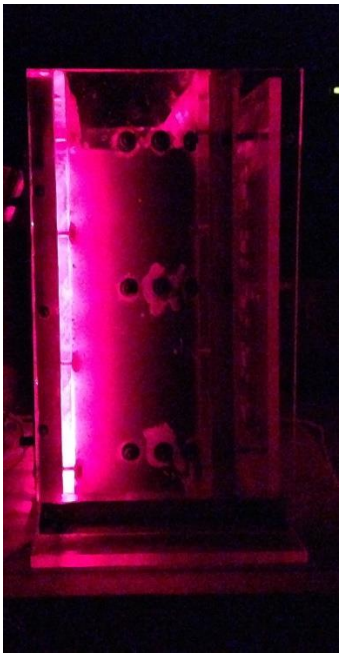

0.81 kg m^{-3}

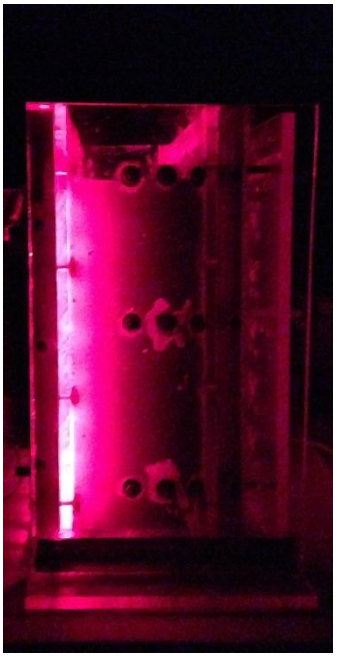

0.73 kg m^{-3}

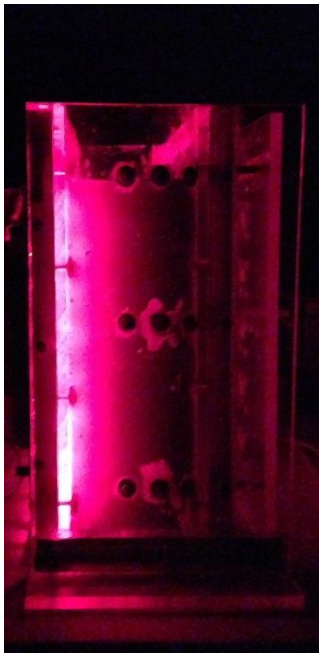

0.58 kg m^{-3}

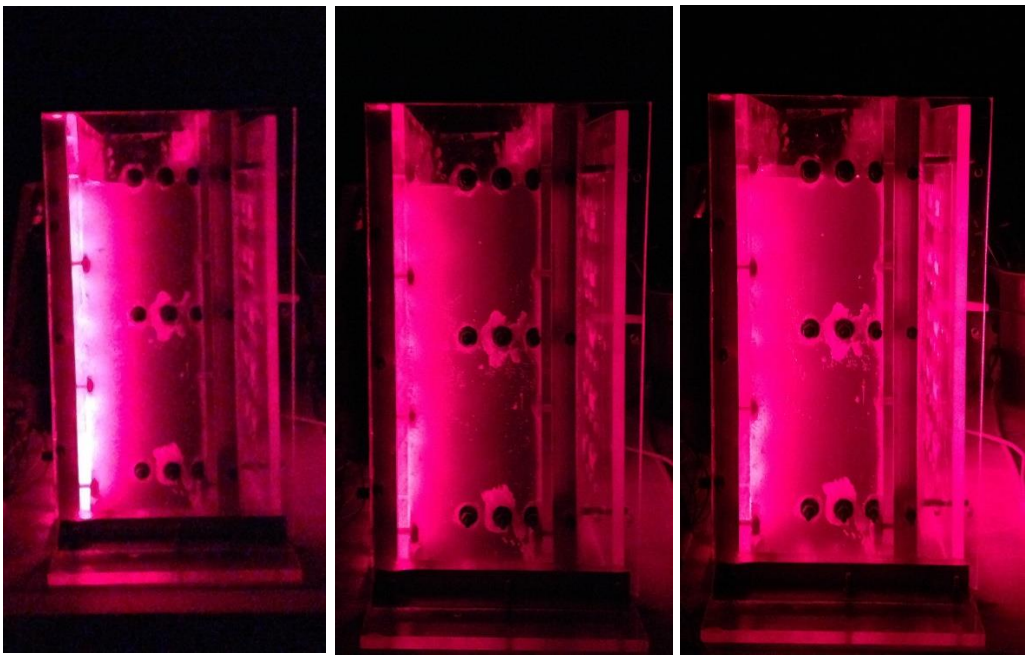

0.47 kg m^{-3} 0.37 kg m^{-3} 0.30 kg m^{-3}

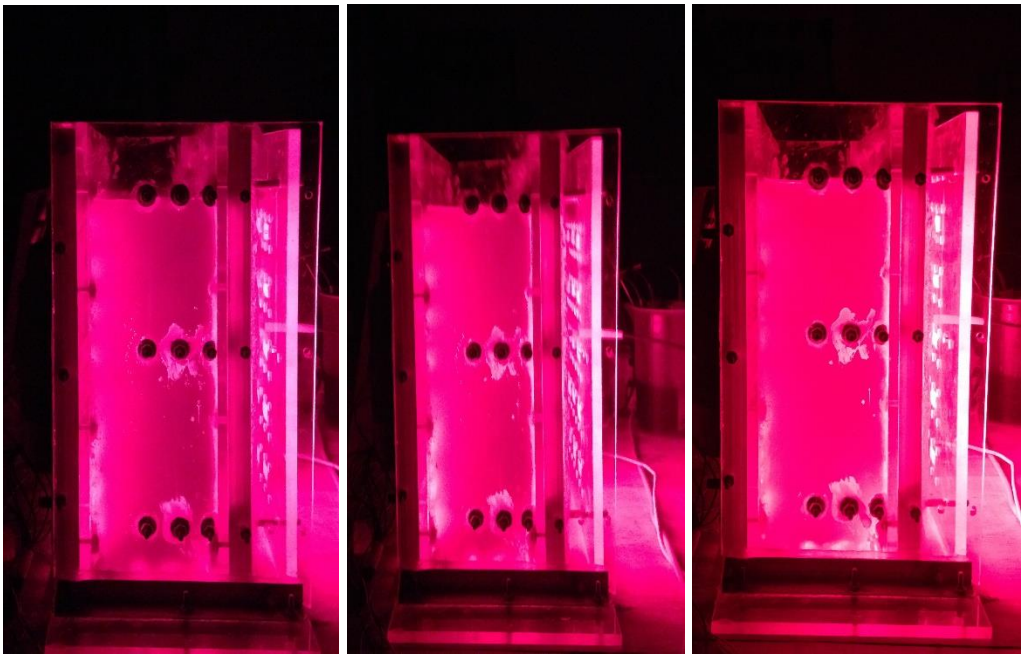

0.24 kg m^{-3} 0.15 kg m^{-3} 0.08 kg m^{-3}